

DEPTH TO THE ARGILLIC HORIZON ON HISTORICALLY FARMED SOIL IN THE
SOUTHEASTERN USA PIEDMONT: SPATIAL MAPPING AND HYDROLOGIC
INFLUENCE

by

RACHEL CAROLAN RYLAND

(Under the Direction of Aaron Thompson and Daniel Markewitz)

ABSTRACT

Throughout the Piedmont of the southeastern USA erosion has transported soil from ridgeline to lower landscape positions. Variations in the depth-to-argillic horizon created by erosion were compared between hillslopes largely undisturbed by agriculture and those with agricultural disturbances. Current patterns in the depth-to-argillic were quantified using soil boring, tile push probe, and electromagnetic induction. Soil boring and tile push showed approximately 40 cm more soil in the lower hillslope on historically farmed land. The depth-to-argillic horizon was predicted using geophysical outputs and regression kriging with 69 % confidence. These data along with saturated hydraulic conductivity measures parameterize hillslope models to investigate variation in topsoil thickness on interflow processes and found that an increase in topsoil depth in lower slope positions may alter lower slope water storage and the hydrologic gradient driving interflow. This research introduces a geophysical method for high resolution soil mapping on previously eroded, forested landscapes.

INDEX WORDS: Erosion, Depth of topsoil, Depth of argillic, Geophysical soil mapping, HYDRUS-2D, Hillslope interflow

DEPTH TO THE ARGILLIC HORIZON ON HISTORICALLY FARMED SOIL IN THE
SOUTHEASTERN USA PIEDMONT: SPATIAL MAPPING AND HYDROLOGIC
INFLUENCE

by

RACHEL CAROLAN RYLAND

B.S., The University of Georgia, 2013

A Thesis Submitted to the Graduate Faculty of The University of Georgia in Partial Fulfillment
of the Requirements for the Degree

MASTER OF SCIENCE

ATHENS, GEORGIA

2017

© 2017

Rachel Carolan Ryland

All Rights Reserved

DEPTH TO THE ARGILLIC HORIZON ON HISTORICALLY FARMED SOIL IN THE
SOUTHEASTERN USA PIEDMONT: SPATIAL MAPPING AND HYDROLOGIC
INFLUENCE

by

RACHEL CAROLAN RYLAND

Major Professors: Aaron Thompson
Daniel Markewitz

Committee: Dorcas Franklin
Charles Rhett Jackson

Electronic Version Approved:

Suzanne Barbour
Dean of the Graduate School
The University of Georgia
December 2017

DEDICATION

My grandfather loved education he was a lifelong student, and school principal. He enjoyed studying social sciences, particularly the history of western civilization, and theology. He fulfilled all requirements to receive a Master's degree in sociology but was unable to pass the Miller Analogies Test to graduate. He, like myself, struggled with a learning disability which held him back from receiving his degree. In honor of Richard Ryland, I would like to dedicate this thesis to him.

ACKNOWLEDGEMENTS

Firstly, I would like to convey my sincere gratitude to my major professors Dr. Daniel Markewitz and Dr. Aaron Thompson for their valuable guidance, and encouragement. My gratitude extends to committee members Dr. Dory Franklin and Dr. Rhett Jackson for their direct influence in my interest, as an undergraduate and graduate student, in natural resources. I would also like to acknowledge Dr. Lori Sutter for the many hours of support in field work and editing, and Dr. David Radcliffe for guidance when working on HYDRUS.

Additionally, I would like to thank my closest friend Carla Gann, for her advice and always lending an ear when I needed one. I would like to acknowledge my lab group members and other UGA staff, Maryam Foroughi, Aaron Joslin, Jill Qi, Caitlin Hodges, Jena Stockton, Matthew Thibodeaux, Elizabeth Osota, Roberto Carrera-Martínez, John Rema, Nehru Mantripragada, and Kim Kauffman for their edits, advice and camaraderie.

My deepest appreciation to my parents for all of their dedication and support throughout every school year. I am grateful for my “editor” (mother), Audrey, who tutored me for countless hours after school. To my incredibly patient father, Bill, for being my constant cheerleader, not only during the time of this thesis, but throughout life. My gratitude extends to my siblings: Erin, Caitlin and Kerry; and Jenifer Monahan, who is a second mother to me, for their support and encouragement over the past couple of years.

TABLE OF CONTENTS

	Page
ACKNOWLEDGEMENTS	v
LIST OF TABLES	viii
LIST OF FIGURES	ix
CHAPTER	
1 INTRODUCTION AND LITERATURE REVIEW	1
References	8
2 MAPPING DEPTH TO THE ARGILLIC HORIZON ON HISTORICALLY FARMED SOIL IN THE SOUTHEASTERN USA PIEDMONT	12
Abstract	13
Introduction	14
Methods	17
Results	23
Discussion	26
Conclusion	29
References	31
3 EVALUATION OF ALTERED DEPTHS TO THE ARGILLIC HORIZON DUE TO EROSION: WHAT IMPACTS ON HILLSLOPE INTERFLOW?	49
Abstract	50
Introduction	51

Methods.....	52
Results.....	59
Discussion.....	61
Conclusion	65
References.....	67
4 CONCLUSION.....	82
APPENDICES	
A ORGANIC MATTER PRETREATMENT	85
B CROSS VALIDATION OF ORDINARY KRIGING FOR GEOPHYSICAL SENSING DATA.....	89
C SAVANNAH RIVER SITE.....	93

LIST OF TABLES

	Page
Table 2.1: Mean depth to the argillic horizon as measured by tile push probe and observed from field soil cores (cm) for historically farmed and reference sites by landscape position in the Calhoun Critical Zone Observatory, SC.	35
Table 2.2: Ordinary least squared regression used to predict the depth-to-clay (from soil core data) for two historically farmed landscapes (Watershed 3 and 4) within the Calhoun Critical Zone Observatory, SC.....	36
Table 2.3: Ordinary least squared regression used to predict the depth-to-clay (using soil core and tile push probe data) for three reference hillslopes (Reference 2, 4, and 9) in the Calhoun Critical Zone Observatory, SC.	37
Table 3.1: Soil water retention parameters for hillslope hydraulic models with uniform and non-uniform topsoil thicknesses.....	68
Table 3.2: Water content contributed by soil horizon for models with uniform and non-uniform topsoil thicknesses	69
Table 3.3: Percent hillslope soil water storage for models with uniform and non-uniform topsoil thicknesses.	70
Table B.1: Cross validation of twenty ordinary kriged surfaces using geophysical sensing data (EMI) for historically farmed watersheds and reference hillslopes; Mean Squared Deviation Ratio (MSDR) and Root Mean Squared Deviation Ratio (RMSR)	89
Table C.1: A spatial error model for the Savannah River Site.	92

LIST OF FIGURES

	Page
Figure 2.1: The Calhoun Critical Zone Observatory research site located within the Sumter National Forest, South Carolina USA.....	38
Figure 2.2: Soil core and tile push probe locations as well as a digital elevation model (DEM) of a) highly eroded, historically farmed watershed showing steep topographical relief and gullying, b) DEM for one of three reference hillslopes (Reference 4) with smooth topographical relief, c) geophysical sensing (EMI) transects in historically farmed and d) reference landscapes.	39
Figure 2.3: Comparison of the depth to the argillic horizon measured by tile push probe (y-axis) and soil auguring (x-axis) for historically farmed (triangle) $R^2 = 0.74$, and reference hillslopes (circle) $R^2 = 0.66$ (the circled measurement was removed before computing correlation).....	40
Figure 2.4: Depth to the argillic horizon along hillslope profile as observed by soil boring (black) and tile push probe (red) in Calhoun Critical Zone Observatory, SC for historically farmed (top, n = 275) and reference landscapes (bottom, n = 122).....	41
Figure 2.5: Cumulative depth response curve (orange) for EMI sensor orientation H2.....	42
Figure 2.6: Comparison of the depth to the argillic horizon predicted by cumulative response curve for EMI sensor orientation H2 (y-axis) and observed depth from soil auguring (x-axis) for previously farmed watershed 3.....	43

Figure 2.7: Predicted depth to the argillic horizon maps created using regression kriging for previously farmed watersheds in the CCZO, SC.....44

Figure 2.8: Predicted depth to the argillic horizon maps created using regression kriging for three reference hillslopes in the CCZO, SC.....45

Figure 2.9: Comparison of the depth to the argillic horizon predicted by regression kriging (y-axis) and observed depth from soil auguring (x-axis) for historically farmed (triangle) $R^2 = 0.69$ and reference hillslopes (circle) $R^2 = 0.27$46

Figure 3.1: Location of the Calhoun Critical Zone Observatory in the Sumter National Forest, SC.....71

Figure 3.2: Precipitation (orange) collected from the Calhoun Critical Zone Observatory (CCZO), and evapotranspiration (blue) collected from weather station near the CCZO for March 1958 to December 1960.....72

Figure 3.3: Boundary conditions and dimensions for vertical hillslope cross section.....73

Figure 3.4: Hillslope soil profile layers for both uniform (top) and non-uniform (bottom) thickness of topsoil74

Figure 3.5: Exponential decrease in rooting distribution parameter for both uniform and non-uniform topsoil thickness models.75

Figure 3.6: Saturated hydraulic conductivity (K_{sat}) measured in 2017 in the Calhoun Critical Zone Observatory on landscapes with uniform and non-uniform thickness of topsoil76

Figure 3.7: Vertical hillslope cross section with particle tracking (grey lines) of interflow, over a two-year simulation, for models with uniform (top) and non-uniform (bottom) topsoil thicknesses.77

Figure 3.8: Simulated daily infiltration, root water uptake, and seepage face flux used to calculate soil water storage for models with uniform and non-uniform topsoil thickness 78

Figure A.1: Soil sample with organic matter (right) and same sample that has been treated with hydrogen peroxide and now appears “bleached” (left).....84

Figure A.2: 1 to 1 correlation of percent clay between samples with organic matter and samples without organic matter (n=9)85

CHAPTER 1

INTRODUCTION AND LITRAETURE REVIEW

This thesis investigates the impacts of erosion in the Piedmont of South Carolina that resulted from an era of land clearing and farming that stretched from approximately 1800-1930. Here I briefly provide some background for Chapter 2 that focuses on mapping the current depth to the argillic horizon that was altered due to this history of erosion and Chapter 3 that endeavors to model the impacts of a change in depth to the argillic horizon on hillslope interflow.

Mapping the Depth to the Argillic Horizon

The southeastern USA Piedmont is approximately 870 miles long and 125 miles wide, extending from New Jersey into Alabama and located between the Appalachian mountain range and the Atlantic Ocean (Golley, 2015). Prior to European settlement in the 1800s, forests dominated this landscape; after settlement, much of the land was largely deforested and converted to agriculture (Trimble, 1974). Deforestation and poor agricultural tillage practices largely conducted to support cotton farming, degraded soil quality in the Piedmont from 1800 to 1930. Damaged and exposed subsurface soil led to compaction and hardening of the surface horizon, thus altering hydrological processes by reducing infiltration. Reduced infiltration coupled with a sloping landscape increased overland flow and promoted soil detachment and erosion (Huang *et al.*, 2002). Accelerated erosion during the cotton farming era resulted in gullies that covered much of the Piedmont after the 1930s (Galang *et al.*, 2007), which further

impacted sediment transportation from upland landscapes to the floodplains and eventually to major rivers and waterways.

Many studies have described the characteristics of elevated sediment transport in the Piedmont that occurred in the cotton farming era (Trimble, 1974; Jackson *et al.*, 2005; Walter *et al.*, 2008; Wegmann *et al.*, 2012; James, 2013). A sediment budget conducted within the Piedmont demonstrated that 12 cm of topsoil was lost from the entire watershed since farming began, and 1.6 m of sediment was deposited on the pre-settlement floodplains (Jackson *et al.*, 2005). These estimates are within the range of other work—using streambank height behind abandoned milldams to estimate sediment load—that suggests 3 to 15 cm of topsoil has been eroded (Wegmann *et al.*, 2012), and 1 to 5 m of sediment has been deposited in the floodplains (Walter *et al.*, 2008; James, 2013). Trimble (1974) estimated that the entire Piedmont region lost up to 30 cm of topsoil.

This redistribution of topsoil has altered the depth to subsurface soil features throughout the Piedmont landscape but a quantitative and spatially explicit mapping of surface soil loss and present subsurface horizon depth has been difficult. Time and cost limit the extent that direct soil sampling (auguring) can be done on large landscapes, which can leave large amounts of landscape under-represented. The tile push probe (TPP), often used in agriculture, is a cost-effective tool that facilitates greater spatial coverage across broader landscapes. In one instance, this probe was used to map changes in depth to the argillic horizon in the Piedmont of South Carolina where over 800 locations were examined on a 5.7 ha hillslope (Du *et al.*, 2016). Although the TPP offers more coverage, this method is still time consuming and, like soil sampling, results in point sample data. Resources, such as the Web Soil Survey, offers easily retrievable soil classification information that can be accessed by numerical modelers for many

types of parameterization for landscape models (*i.e.* depth to the argillic horizon, soil textural classes, bulk density, *etc.*). Parameterization from soil classification resources may not accurately represent landscapes that have been highly eroded such as those in the Calhoun Critical Zone Observatory. A quick and non-invasive technique for determining detailed spatial variations in soil properties (*i.e.*, depth of A or depth to B) over large areas that have been highly eroded, therefore, would be valuable.

Geophysical sensing devices such as ground penetrating radar (GPR) and electromagnetic induction (EMI) offer non-invasive techniques that have been used in agriculture and natural resource mapping since the 1970s (Doolittle *et al.*, 2014). These are popular instruments due to their relative cost effectiveness, and they provide insight into subsurface physical properties without having to penetrate the soil - giving them the capability to cover large areas within a short time frame. Unlike soil sampling and TPP, tens of thousands of measurements can be made daily with geophysical devices, leading to a higher resolution of spatial sampling in the landscape. The type of geophysical instrument used depends on site characteristics (*i.e.*, relief, vegetation coverage, *etc.*) and the desired depth of investigation. The depth of investigation of a particular geophysical instrument is limited by the number, spacing, and frequency of the sensors. GPR generally has one sensor that can be set to multiple frequencies increasing the depth at which the measurement is taken, but each frequency measures only one depth, requiring multiple passes over the same area for deep profile investigation (De Benedetto *et al.*, 2012). EMI can offer greater flexibility, due to the number and spacing of sensors such that multiple frequencies can be measured in a single pass for integrated measurements of the whole soil profile. In contrast to GPR that is typically pulled along the ground, EMI instruments can be held above the ground making it easier to navigate through low, thick understory or over fallen trees

and is, thus, well suited for forested watersheds. In addition, EMI devices are an indirect indicator of soil chemical and physical properties (*i.e.*, clay content), and have primarily been used in precision agriculture to map variations in shallow soil properties for optimizing crop production (Sudduth *et al.*, 2001; Corwin *et al.*, 2003; Corwin *et al.*, 2005; Grisso *et al.*, 2005; Shanahan *et al.*, 2015). Other studies have mapped deeper soil profiles in agricultural fields to predicted soil texture (clay content) with depth using EMI (Rhoades *et al.*, 1989; Sudduth *et al.*, 2003; Sudduth *et al.*, 2010; Heil *et al.*, 2012; White *et al.*, 2012).

Saey *et al.* (2011) found that a DUALEM-21S could predict the depth to the top of the argillic horizon with 95 % confidence using the cumulative depth response curve (CRC) method on a homogenous loess capped argillic horizon in Belgium. In the Piedmont, the absence of a distinct and uniform interface between topsoil and subsoil, as in Belgium, may create some measurement difficulties of depth to the argillic horizon in these heterogeneous soils (Li *et al.*, 2010). On the other hand, Sudduth *et al.* (2013) found that geophysical sensing measurements that had large (≥ 3.3 mS/m) standard deviations proved beneficial when fitting a response curve and predicting depth-to-clay. Also, it may be possible that the absolute depth of the argillic may affect the prediction ability as the response of the geophysical sensing devices generally declines with depth (McNeill, 1980). For example, a previous study in the farmlands of the Tertiary hills of Southern Germany where clays are surficial (*i.e.*, <50 cm) used linear regression to predict clay content with 76 % confidence using electrical conductivity (Heil *et al.*, 2012). In contrast, working in deeper Vertisols on floodplains in New South Wales, Australia clay content was only 32 % correlated with inverse EMI data (Triantafilis *et al.* 2013a, b). Little work with geophysical sensing has been done in upland forested Piedmont landscapes; one study showed that percent clay in the top 30 cm was 73 % correlated with geophysical sensing data on Mollisol covered

hillslopes of Reynolds Mountain Experimental Watershed in Idaho (Robinson *et al.*, 2008).

Chapter 2 of this thesis aimed to improve our understanding of erosion on sediment redistribution in upland forested Piedmont hillslopes by mapping spatial variations in the depth to the argillic horizon. Since the depth to the argillic horizon, within the CCZO and across the Piedmont, has been disturbed by agriculture practices, these landscapes may not be accurately represented by resources such as the Web Soil Survey. When parameters such as the depth to the argillic horizon are extracted from the Web Soil Survey for model parameterization the model again may not represent landscapes and lead to error in model estimations. Therefore, the potential use of geophysical sensing (specifically EMI) was investigated as an accurate and efficient means of measuring the depth to the argillic horizon in this forested landscape. I hypothesized that: 1) the mean depth to the argillic horizon would be shallower along the ridges and deeper throughout lower slopes in the historically farmed landscapes than in the undisturbed reference landscapes, and 2) geophysical sensing using a dual- receiver EMI would be an accurate ($R^2 \geq 0.60$) means for predicting depth to the argillic horizon on upland forested soils with a history of farming. I tested these hypotheses by measuring the depth to the argillic using direct soil auguring, TPP, and dual- receiver EMI across upland forest soils of the South Carolina Piedmont, which contain both land areas that have been previously farmed and a few that, although the trees were previously harvested, were relatively undisturbed.

Hillslope Hydrology

Based on the observed differences in depth to the argillic horizon in reforested and reference hillslopes described in Chapter 2 of this thesis I tried to quantify, through model simulation, how these differences might influence hillslope hydrology. Hillslope hydrology of

the Piedmont typically involves an argillic horizon with low permeability causing high lateral flow (on top of or within the argillic horizon) in periods of high precipitation (Dreps, 2011). Accelerated erosion in this region has resulted in soil redistribution from upper to lower landscape positions (Gabbard *et al.*, 1998), compared to landscapes with minimal agricultural disturbance which tend to have a nearly consistent depth of topsoil. Such redistribution is rarely accounted for in efforts to model hillslope and watershed hydrology.

Numerical models of hillslope and watershed hydrology typically have estimated topsoil thickness either from soil classification maps (Dialynas *et al.*, 2016) or digital elevation models (Quinn *et al.*, 1991; Paniconi *et al.*, 1993), or they have approximated a topsoil thickness parallel to the soil surface (O'loughlin, 1981; Jackson *et al.*, 2014). To quantify hillslope interflow, these approximations may lack sufficient spatial detail and may not accurately represent non-uniform subsoil topographies where different zones of interflow occur on low permeability, argillic horizons (Du *et al.*, 2016). Studies have shown that non-parallel topographies of hydraulically limiting subsoil can cause variation in water content along the hillslope (*i.e.* perched water table) as opposed to uniform topsoil thicknesses, which creates infrequent interflow events (Chaplot *et al.*, 2003; Ali *et al.*, 2011; Du *et al.*, 2016). Therefore, a spatially explicit hillslope model containing a non-uniform topsoil thickness could create zones of interflow that are different than current estimates that use uniform topsoil thickness to argillic horizons.

Chapter 3's objective was twofold. First, I quantified differences in field saturated hydraulic conductivity across Piedmont landscapes with evidence of historic farming and erosion (non-uniform depth to clay) relative to others that did not show evidence of farming (uniform depth-to-clay). Second, I used these measurements as well as other site characteristics (*i.e.* depth-to-argillic, root distribution, climate data) to parameterize two HYDRUS 2D computational

models, one for each depth-to-clay scenario (uniform and non-uniform). A comparison of the hillslope hydrology between uniform and non-uniform models was conducted with particle tracking (to visualize interflow pathways), variations in water content, and a water budget at the end of a two-year simulation to determine net soil water storage. I hypothesized that interflow would be higher in the uniform depth-to-clay hillslope and soil water storage would be lower due to the thinner topsoil thickness at the toe-slope, compared to the non-uniform depth-to-clay model.

References

- Ali, G. A., L'Heureux, C., Roy, A. G., Turmel, M.-C., & Courchesne, F. (2011). Linking spatial patterns of perched groundwater storage and stormflow generation processes in a headwater forested catchment. *Hydrological Processes*, 25(25), 3843-3857. doi:10.1002/hyp.8238
- Chaplot, V., & Walter, C. (2003). Subsurface topography to enhance the prediction of the spatial distribution of soil wetness. *Hydrological Processes*, 17(13), 2567-2580. doi:10.1002/hyp.1273
- Corwin, D., & Lesch, S. (2005). Apparent soil electrical conductivity measurements in agriculture. *Computers and electronics in agriculture*, 46(1), 11-43.
- Corwin, D., Lesch, S., Shouse, P., Soppe, R., & Ayars, J. (2003). Identifying soil properties that influence cotton yield using soil sampling directed by apparent soil electrical conductivity. *Agronomy Journal*, 95(2), 352-364.
- De Benedetto, D., Castrignano, A., Sollitto, D., Modugno, F., Buttafuoco, G., & Papa, G. I. (2012). Integrating geophysical and geostatistical techniques to map the spatial variation of clay. *Geoderma*, 171-172, 53-63. doi:10.1016/j.geoderma.2011.05.005
- Dialynas, Y. G., Bastola, S., Bras, R. L., Billings, S. A., Markewitz, D., & Richter, D. d. (2016). Topographic variability and the influence of soil erosion on the carbon cycle. *Global Biogeochemical Cycles*, 30(5), 644-660. doi:10.1002/2015GB005302
- Doolittle, J. A., & Brevik, E. C. (2014). The use of electromagnetic induction techniques in soils studies. *Geoderma*, 223, 33-45.
- Dreps, C. L. (2011). Water Storage Dynamics and Water Balances of Two Piedmont North Carolina Headwater Catchments (Master's Thesis). NC State University, Raleigh, North Carolina.
- Du, E., Jackson, C. R., Klaus, J., McDonnell, J. J., Griffiths, N. A., Williamson, M. F., Greco, J. L., & Bitew, M. (2016). Interflow dynamics on a low relief forested hillslope: Lots of fill, little spill. *Journal of Hydrology*, 534, 648-658.

- Gabbard, D., Huang, C., Norton, L., & Steinhardt, G. (1998). Landscape position, surface hydraulic gradients and erosion processes. *Earth Surface Processes and Landforms*, 23(1), 83-93.
- Galang, M., Markewitz, D., Morris, L., & Bussell, P. (2007). Land use change and gully erosion in the Piedmont region of South Carolina. *Journal of Soil and Water Conservation*, 62(3), 122-129.
- Grisso, R. D., Alley, M. M., Holshouser, D. L., & Thomason, W. E. (2009). Precision Farming Tools. Soil Electrical Conductivity. Available from: <http://pubs.ext.vt.edu/442/442-508/442-508.html>.
- Golley, Frank B. (2004). Piedmont Geographic Region. <http://www.georgiaencyclopedia.org/articles/geography-environment/piedmont-geographic-region>
- Heil, K., & Schmidhalter, U. (2012). Characterisation of soil texture variability using the apparent soil electrical conductivity at a highly variable site. *Computers & Geosciences*, 39, 98-110.
- Huang, C., Gascuel-Oudou, C., & Cros-Cayot, S. (2002). Hillslope topographic and hydrologic effects on overland flow and erosion. *CATENA*, 46(2-3), 177-188.
doi:[http://dx.doi.org/10.1016/S0341-8162\(01\)00165-5](http://dx.doi.org/10.1016/S0341-8162(01)00165-5)
- Jackson, C. R., Bitew, M., & Du, E. (2014). When interflow also percolates: downslope travel distances and hillslope process zones. *Hydrological Processes*, 28(7), 3195-3200.
- Jackson, C. R., Martin, J. K., Leigh, D. S., & West, L. T. (2005). A southeastern piedmont watershed sediment budget: Evidence for a multi-millennial agricultural legacy. *Journal of Soil and Water Conservation*, 60(6), 298-310.
- James, L. A. (2013). Legacy sediment: Definitions and processes of episodically produced anthropogenic sediment. *Anthropocene*, 2, 16-26.
doi:<http://dx.doi.org/10.1016/j.ancene.2013.04.001>
- Li, J., Mendoza, A., & Heine, P. (2010). Effects of land-use history on soil spatial heterogeneity of macro-and trace elements in the Southern Piedmont USA. *Geoderma*, 156(1), 60-73.

- McNeill, J. (1980). Electromagnetic terrain conductivity measurement at low induction numbers. Geonics Technical Notes. TN - 6. 15 pp: Geonics Limited Ontario, Canada.
- O'loughlin, E. (1981). Saturation regions in catchments and their relations to soil and topographic properties. *Journal of Hydrology*, 53(3-4), 229-246.
- Paniconi, C., & Wood, E. F. (1993). A detailed model for simulation of catchment scale subsurface hydrologic processes. *Water Resources Research*, 29(6), 1601-1620.
- Quinn, P., Beven, K., Chevallier, P., & Planchon, O. (1991). The prediction of hillslope flow paths for distributed hydrological modelling using digital terrain models. *Hydrological Processes*, 5(1), 59-79.
- Rhoades, J., Manteghi, N., Shouse, P., & Alves, W. (1989). Soil electrical conductivity and soil salinity: New formulations and calibrations. *Soil Science Society of America Journal*, 53(2), 433-439.
- Robinson, D. A., Abdu, H., Jones, S. B., Seyfried, M., Lebron, I., & Knight, R. (2008). Eco-geophysical imaging of watershed-scale soil patterns links with plant community spatial patterns. *Vadose Zone Journal*, 7(4), 1132-1138.
- Saey, T., Van Meirvenne, M., De Smedt, P., Cockx, L., Meerschman, E., Islam, M. M., & Meeuws, F. (2011). Mapping depth-to-clay using fitted multiple depth response curves of a proximal EMI sensor. *Geoderma*, 162(1), 151-158.
- Shanahan, P. W., Binley, A., Whalley, W. R., & Watts, C. W. (2015). The use of electromagnetic induction to monitor changes in soil moisture profiles beneath different wheat genotypes. *Soil Science Society of America Journal*, 79(2), 459-466.
- Sudduth, K., Drummond, S., & Kitchen, N. (2001). Accuracy issues in electromagnetic induction sensing of soil electrical conductivity for precision agriculture. *Computers and electronics in agriculture*, 31(3), 239-264.
- Sudduth, K., Kitchen, N., Bollero, G., Bullock, D., & Wiebold, W. (2003). Comparison of electromagnetic induction and direct sensing of soil electrical conductivity. *Agronomy Journal*, 95(3), 472-482.

- Sudduth, K. A., Kitchen, N. R., Myers, D. B., & Drummond, S. T. (2010). Mapping depth to argillic soil horizons using apparent electrical conductivity. *Journal of Environmental & Engineering Geophysics*, 15(3), 135-146.
- Sudduth, K. A., Myers, D. B., Kitchen, N. R., & Drummond, S. T. (2013). Modeling soil electrical conductivity–depth relationships with data from proximal and penetrating ECa sensors. *Geoderma*, 199, 12-21.
- Trimble, S. W. (1974). Man-induced soil erosion on the southern Piedmont. *Soil Conserv. Soc. Am., Ankeny, Iowa, 1700-1970*.
- Triantafyllis, J., Terhune, C., & Santos, F. M. (2013a). An inversion approach to generate electromagnetic conductivity images from signal data. *Environmental modelling & software*, 43, 88-95.
- Triantafyllis, J., & Santos, F. M. (2013b). Electromagnetic conductivity imaging (EMCI) of soil using a DUALEM-421 and inversion modelling software (EM4Soil). *Geoderma*, 211, 28-38.
- Walter, R. C., & Merritts, D. J. (2008). Natural streams and the legacy of water-powered mills. *Science*, 319(5861), 299-304.
- Wegmann, K. W., Lewis, R. Q., & Hunt, M. C. (2012). Historic mill ponds and piedmont stream water quality: Making the connection near Raleigh, North Carolina. *Field Guides*, 29, 93-121.
- White, M. L., Shaw, J. N., Raper, R. L., Rodekohr, D., & Wood, C. W. (2012). A multivariate approach for high-resolution soil survey development. *Soil science*, 177(5), 345-354.

CHAPTER 2

MAPPING DEPTH TO THE ARGILLIC HORIZON ON HISTORICALLY FARMED SOIL IN THE SOUTHEASTERN USA PIEDMONT¹

¹Ryland, R. C., D. Markewitz, and A. Thompson. 2017. To be submitted to *Geoderma*.

Abstract

The Piedmont region of the southeastern United States experienced a period of accelerated erosion in the 1800s. Clear-cutting of the forests coupled with soil tilling and inadequate erosion control practices led to substantial soil redistribution and loss. This redistribution exposed the subsoil clay (argillic) horizon in many locations and adversely altered the hydrologic processes across the landscape. Understanding current hydrologic and biogeochemical processes in this landscape requires an accurate assessment of this soil redistribution and the current depth to the argillic horizon. To achieve this mapping, the depth to the argillic horizon was measured in highly eroded (historically farmed) and undisturbed hillslopes (reference areas). In addition to directly measuring the depth to the argillic by soil auguring, and tile push probing we made geophysical measurements via electromagnetic induction (EMI) to assess our ability to predict the depth to the argillic horizon remotely. Combining these measurements with site topographic characteristics (*i.e.* landscape position, aspect, percent slope) we generated predictive models of the depth to the argillic horizon. Direct measures indicated that historically farmed watersheds, although reforested since the 1930s, had significant soil redistribution present (p -value = 0.0521) in the toe-slope position compared to reference landscapes which had fairly consistent depths. Our data suggests geophysical sensing is an efficient means of predicting depth-to-clay on previously farmed sites when combined with landscapes feature characteristics ($R^2 = 0.69$); however, caution should be used when selecting these characteristics, as they may not represent all land use types.

Introduction

The southeastern USA Piedmont is approximately 870 miles long and 125 miles wide, extending from New Jersey into Alabama and located between the Appalachian mountain range and the Atlantic Ocean (Golley, 2015). Prior to European settlement in the 1800s, forests dominated this landscape; after settlement, much of the land was largely deforested and converted to agriculture (Trimble, 1974). Deforestation and poor agricultural tillage practices largely conducted to support cotton farming, degraded soil quality in the Piedmont from 1800 to 1930. Damaged and exposed subsurface soil led to compaction and hardening of the surface horizon, thus altering hydrological processes by reducing infiltration. Reduced infiltration coupled with sloping landscape increased overland flow and promoted soil detachment and erosion (Huang *et al.*, 2002). Accelerated erosion during the cotton farming era resulted in gullies that covered much of the Piedmont after the 1930s (Galang *et al.*, 2007), which further impacted sediment transportation from upland landscapes to the floodplains and eventually to major rivers and waterways.

Many studies have described the characteristics of elevated sediment transport in the Piedmont that occurred in the cotton farming era (Trimble, 1974; Jackson *et al.*, 2005a; Walter *et al.*, 2008; Wegmann *et al.*, 2012; James, 2013). A sediment budget conducted within the Piedmont demonstrated that 12 cm of topsoil was lost from the entire watershed since farming began, and 1.6 m of sediment was deposited on the pre-settlement floodplains (Jackson *et al.*, 2005a). These erosion estimates are within the range of other work—using streambank height behind abandoned milldams to estimate sediment load—that suggests 3 to 15 cm of topsoil has been eroded (Wegmann *et al.*, 2012), and 1 to 5 m of sediment has been deposited in the

floodplains (Walter *et al.*, 2008; James, 2013). Trimble (1974) estimated that the entire Piedmont region lost up to 30 cm of topsoil.

This redistribution of topsoil has altered the depth to subsurface soil features throughout the Piedmont landscape but a quantitative and spatially explicit mapping of surface soil loss and present subsurface horizon depth has been difficult. Time and cost limit the extent that direct soil sampling (auguring) can be done on large landscapes, which can leave large amounts of landscape under-represented. The tile push probe (TPP), often used in agriculture, is a cost-effective tool that facilitates more spatial coverage across broader landscapes. In one instance, this probe was used to map changes in depth to the argillic horizon in the Piedmont of South Carolina where over 800 locations were examined on a 5.7 ha hillslope (Du *et al.*, 2016). Although the TPP offers more coverage, this method is still time consuming and, like soil sampling, results in point sample data. A quick and non-invasive technique for determining detailed spatial variations in soil properties (*i.e.*, depth of A or depth to B) over large areas, therefore, would be valuable.

Geophysical sensing such as ground penetrating radar (GPR) and electromagnetic induction (EMI) offer non-invasive techniques that have been used in agriculture and natural resource mapping since the 1970s (Doolittle *et al.*, 2014). These are popular instruments due to their relative cost effectiveness, and they provide insight into subsurface physical properties without having to physically penetrate the soil - giving them the capability to cover large areas within a short time frame. Unlike soil sampling and TPP, tens of thousands of measurements can be made daily with geophysical devices, leading to a higher resolution of spatial sampling in the landscape. The type of geophysical instrument used depends on site characteristics (*i.e.*, relief, vegetation coverage, etc.) and the desired depth of investigation. The depth of investigation of a

particular geophysical instrument is limited by the number, spacing, and frequency of the sensors. GPR generally has one sensor that can be set to multiple frequencies increasing the depth at which the measurement is taken, but each frequency measures only one depth, requiring multiple passes over the same area for deep profile investigation (De Benedetto *et al.*, 2012). EMI can offer greater flexibility, due to the number and spacing of sensors, such that multiple frequencies can be measured in a single pass for integrated measurements of the whole soil profile. In contrast to GPR that is typically pulled along the ground, EMI instruments can be held above the ground making it easier to navigate through low, thick understory or over fallen trees and is, thus, well suited for forested watersheds. In addition, EMI devices are an indirect indicator of soil chemical and physical properties (*i.e.*, clay content), and have primarily been used in precision agriculture to map variations in shallow soil properties for optimizing crop production (Sudduth *et al.*, 2001; Corwin *et al.*, 2003; Corwin *et al.*, 2005; Grisso *et al.*, 2005; Shanahan *et al.*, 2015). Other studies have mapped deeper soil profiles in agricultural fields to predicted soil texture (clay content) with depth using EMI (Rhoades *et al.*, 1989; Sudduth *et al.*, 2003; Sudduth *et al.*, 2010; Heil *et al.*, 2012; White *et al.*, 2012)

This study aimed to improve our understanding of erosion on sediment redistribution in upland forested Piedmont hillslopes by mapping spatial variations in the depth to the argillic horizon. We sought to assess the potential use of geophysical sensing (specifically EMI) as an accurate and efficient means of measuring the depth to the argillic horizon in this forested landscape. We hypothesized that: 1) the mean depth to the argillic horizon would be shallower along the ridges and deeper throughout lower slopes in the historically farmed landscapes than in the undisturbed reference landscapes, and 2) geophysical sensing using a dual-receiver EMI would be an accurate ($R^2 \geq 0.60$) means for predicting depth to the argillic horizon on upland

forested soils with a history of farming. We tested these hypotheses by measuring the depth to the argillic using direct soil auguring, TPP, and dual-receiver EMI across upland forest soils of the South Carolina Piedmont, which contain both land areas that have been previously farmed and a few that, although the trees were previously harvested, were relatively undisturbed.

Methods

Study Site

The Calhoun Critical Zone Observatory (CCZO) is located within the Sumter National Forest, in the Piedmont region of South Carolina (Figure 2.1). The CCZO mission involves a collaborative effort to evaluate the influence of past anthropogenic activities on soil degradation and how these ecosystems have evolved since agricultural abandonment (Richter *et al.*, 2015). The formerly hardwood ecosystem was clear-cut and tilled for agricultural purposes in the early 1800s, resulting in soil degradation and high erosion rates. Eventually, for a range of natural, economic, and social factors, these agricultural lands were abandoned (Coughlan *et al.*, 2017). In the 1930s much of the area within the CCZO that was previously degraded by agricultural use was abandoned. Since abandonment, natural reforestation has occurred and some areas were planted in pine, which currently covers most of the landscapes; these efforts have improved soil quality (Richter *et al.*, 2001; Richter *et al.*, 2015).

Land use history in the CCZO has been partly reconstructed from land deeds and aerial photographs (Richter *et al.*, 2001; Coughlan *et al.*, 2017). Some agricultural clearings can be identified on 1933 aerial photographs of the CCZO taken near the time of abandonment (circa 1950) (Brecheisen *et al.*, 2015). Similarly, certain areas of forested hardwoods during that time are visible, and combined with recent high-resolution (1 m²) LIDAR (NCALM, 2016) indicate a

history lacking agriculture and gulley erosion. From this information, two watersheds (Watershed 3 and 4 and hereafter referred to as “historically farmed”) that were previously cleared for agriculture and part of an erosion control study in the 1950s (Metz, 1958) and three hillslopes (Reference 2, 4, or 9 and hereafter referred to as “references”) that were under hardwood forest and have been minimally disturbed were identified for this study. There was an absence of terracing in both land use types. The typical soil order for these watersheds is Ultisols with minor inclusions of Alfisols, which in an un-eroded state both have a sandy surface horizon with a clay subsoil; soil series include Cecil, Madison and Wilkes (Richter *et al.*, 2000).

Soil Sampling

Soil borings were used to investigate the spatial variations in the depth-to-argillic layer. The soil profiles were augured to 200 cm and sampled at seven depth intervals (0-7.5, 7.5-15, 15-35, 35-60, 60-100, 100-150, and 150-200 cm) based on prior studies within the area or until the argillic horizon was reached (Richter *et al.*, 1994; Richter *et al.*, 2000). Soil samples were collected along transects following the hillslope profile within reforested and reference landscapes. The transects were distributed from north to south and oriented perpendicular to the direction of stream flow. Three transects were evaluated in each watershed (upstream, midstream, and downstream) with 10 sample locations per transect and three sample locations on each reference hillslope (Figure 2.2). In total, 82 cores were collected along the hillslopes within each watershed, and 9 from the reference hillslopes. Particle size analysis following the methods of Gee *et al.* (2002) determined clay content for each sample depth collected. Detailed particle size data for this research can be found at Ryland (2017). Organic matter was not removed from surface soil samples prior to particle size analysis as the removal of organic matter did not

significantly change the samples clay percentage (See APPENDIX A) The depth-to-argillic horizon by landscape position was tested for significant differences between land use types by T-test comparison (JMP[®], Version Pro 13.0.0. SAS Institute Inc., Cary, NC, 1989-2007).

Tile Push Probes

In addition to bored soil samples, the depth-to-argillic layer was determined via TPP at 223 locations within each watershed and 52 locations in reference areas (Figure 2.2). The TPP was calibrated by estimating the depth to the argillic horizon next to all bored soil samples prior to augering. The TPP are 1 to 2 m in length and consist of a thin steel rod with a sharpened end. Like a penetrometer, the TPP are sensitive to changes in soil density as it is pushed into the ground, TPP exert a high resistance when the tip of the probe is at the argillic interface. The TPP were pressed into the ground with 3 to 5 replications within an approximately 8.0 cm diameter circle, and the deepest probe depth was recorded as the depth to the argillic horizon (Du *et al.*, 2016). Both the soil borings and push probe data were geo-referenced with an Archer 2 GPS unit (Juniper System Inc., Logan, UT, USA)

Electromagnetic Induction Survey and Instrumentation

Detailed measurements of soil electrical conductivity were taken using an electromagnetic induction (EMI) sensor. A Dualem-21S EMI instrument (Dualem Inc., Milton, ON, Canada) was utilized to record the apparent electrical conductivity of the soil in each watershed and hillslope. Apparent electrical conductivity of bulk soil is a function of many soil properties, such as bulk density and cation exchange capacity, but in this environment it is primarily responsive to soil moisture and clay content (Weller *et al.* 2007; Robinson *et al.*,

2008). Clay soil contains a higher moisture content than sandier textures, therefore, the electrical conductivity will be higher in clay-rich soils. The EMI sensor was carried at a height of 40 cm above the ground along transects from ridge to toe-slope at 5 to 7 m contours across the watershed (Figure 2.2).

The Dualem 21S EMI utilizes a transmitter that sends a high frequency (9000Hz) eddy current into the soil where it interacts with various soil properties (i.e. texture, moisture, temperature, etc.) that induce a secondary current (Doolittle *et al.*, 2014). This secondary current is detected by two receivers (i.e., dual-receiver) located at 1.0 m and 2.0 m spacing along the instrument's horizontal axis. Each receiver has two coil orientations, perpendicular geometry (P1 and P2) and a horizontal co-planar (H1 and H2) geometry. This quadruple configuration allows for a high resolution of the apparent electrical conductivity within the soil profile up to 3.0 m in depth, depending on instrument height above the ground. The secondary current is detected by the receiver(s) as low induction numbers (LIN), which corresponds to the apparent electrical conductivity of the soil (McNeill, 1980). LIN data were logged using an Archer 2 GPS unit (Juniper System Inc., Logan, UT, U.S.A.) with SensorTrac and handheld Geographic Information Systems software (StarPal, Fort Collins, CO, U.S.A.).

Ordinary Kriging and Cross Validation

Electrical conductivity data, collected by the EMI instrument, was kriged into continuous surfaces, this was to ensure overlap between electrical conductivity data and sampling points from soil boring and TPP. Electrical conductivity was extracted at each sampling point and later used for regression purposes. Prior to kriging, electrical conductivity data generated with the EMI were filtered to remove negative values, which represent background interference, as well

as high values that are outliers and presumed to be unseen metal (e.g. pin flags, bullet casings). The average upper limit for high values was 10.9 mS m^{-1} but this limit changed slightly with each orientation of the EMI sensor (*i.e.*, 3.4 to 27.5 mS m^{-1}). This filtering resulted in the removal of 17 % of the raw data before analysis.

Using these filtered data, the distribution was evaluated for normality and log transformed prior to kriging if needed. Twenty ordinary kriged surfaces were created for this study, representing the four orientations of the EMI sensors (P1, P2, H1, and H2) in each of the five different study areas (Watersheds 3 and 4 and Reference Hillslopes 2, 4 and 9). Ordinary kriging of the geophysical sensing data was conducted using the Geostatistical Wizard tool in ArcGIS (ESRI, Redlands, CA, USA). Assumptions for ordinary kriging include a spherical semi-variogram model with anisotropy and directionality. The lag size and lag number varied with each prediction map as the size of the study area changed depending on the site. Generally, the farthest distance between geophysical sensing transects were determined by the measuring tool in ArcGIS, and the lag size was approximately half that distance. Cross validation, using 10 % of the geophysical sensing data, of the twenty ordinary kriged surfaces was conducted to test model performance. Overall, the ordinary kriging was a good fit, and provided accurate results for 3 of the 4 EMI sensor orientations as well 4 of the 5 study sites (APPENDIX B).

Soil boring and TPP locations were overlaid on these kriged surfaces and electrical conductivity values from all orientations were obtained using the extraction tool in ArcGIS. The measurements of depth-to-argillic from soil boring and TPP along with the extracted EMI measurements formed the basis of the cumulative response curve, multivariate regressions, and regression kriging approaches described below.

Analysis of Geophysical Sensing

The depth to the top of the argillic horizon was predicted using a cumulative depth response curve (CRC, a power function) that relates the depth to the top of the argillic horizon to electrical conductivity measurements (Saey *et al.*, 2011). Parameters α and β in the power function were empirically determined by minimizing the sum of squared differences between the observed and predicted depths to the top of the argillic horizon. The cumulative response function for the horizontal co-planar (H1 and H2) EMI orientations is shown below:

$$R_H = \alpha_H \cdot e^{-\beta_H \cdot \left(\frac{Z_{Clay}}{S}\right)} \quad \text{Equation 3.1}$$

with R_H representing the response of the electrical conductivity reading above the depth of clay (Z_{Clay}) for the horizontal co-planar EMI orientation with instrument spacing S . Unknown exponential parameters α_H and β_H are solved for by an iterative process.

In addition to the single variate CRC method, a multivariate ordinary least square regression (OLS) was utilized for regression kriging purposes (Hengl *et al.*, 2007). In regression kriging, as a first step, a multivariate linear regression is developed to explain variation in the dependent variable of interest (*e.g.*, depth-to-argillic) based on available independent variables (Worsham *et al.*, 2012). In this study, the independent variables included all the EMI orientations (*i.e.*, P1, P2, H1, H2) as well as logically derived conductivity variables, in other words deeper conductivity measures minus shallower measures (*i.e.*, H1-P1, P2-P1, H2-P1, P2-H1, H2-H1, and H2-P2). Finally, slope, aspect, and landscape position (*i.e.*, ridge, shoulder, mid-slope, toe-slope, and foot-slope) extracted from a DEM (resolution 1 m²) for the measured areas were all included in the multivariate regression.

Using these variables, a multivariate regression model was developed for each land use type: historically farmed watersheds and reference hillslopes. A p-value of ≤ 0.15 was used to allow explanatory variables into the model and $R^2 \geq 0.60$ was the criteria used to suggest a model had meaningful predictive utility. Regression equations were determined in the GeoDa spatial software package (The University of Chicago, Illinois, U.S.A). Based on the multivariate regressions for the different land uses, prediction residuals were obtained for each soil boring or TPP measurement within each site.

These site and location-specific residuals as well as the other significant explanatory variables were imported into ArcGIS (ESRI, Redlands, CA, U.S.A.) and kriged (i.e., residual – simple kriging, landscape position – indicator kriging, and EMI outputs – ordinary kriging) to create rasters with a cell size of 1 m^2 that could be used for prediction. The raster calculator tool within ArcGIS was then used to run the multivariate regression model to predict depth-to-argillic and then added or subtracted to the residual prediction error to generate a final prediction map for each site.

Results

Soil Sampling and Tile Push Probe

The depth to the argillic horizon, determined by TPP, correlated strongly with soil boring observations for historically farmed watersheds ($R^2 = 0.74$); however, the TPP underestimated the depth to the argillic layer whenever the layer was deeper than 100 cm. In reference landscapes, a similar relationship exists but with a weaker correlation ($R^2 = 0.66$; Figure 2.3). The mean depth to the argillic horizon by landscape position as measured by TPP and observed by soil borings in the field for historically farmed watersheds and in reference hillslopes differed

(Table 2.1). The depth to the argillic horizon in the historically farmed landscapes ranged from 26 (± 2.36) to 87 (± 12.38) cm while in the reference hillslopes only ranged from 30 (± 3.09) to 48 (± 12.50) cm (Table 2.1). The standard deviation in depth to the argillic horizon for historically farmed sites increased from ridge to toe-slope. In the reference landscapes, however, the standard deviation decreased from ridge to mid-slope and increased again to toe-slope. Soil boring and TPP measures indicated that historically farmed watersheds had significantly redistributed soil in the mid-slope (p-value = 0.0012) and toe-slope (p-value = 0.0521) landscape position compared to reference hillslopes with fairly consistent depths-to-argillic (Figure 2.4).

Analysis of Geophysical Sensing

The CRC method could not be successfully applied to the reference hillslopes as there was minimal variation in the depth to the argillic horizon such that the response curve was flat and poorly fit the data. In the historically farmed landscapes, the H2 orientation had the best relationship between the geophysical sensing data and depth-to-clay, thus a CRC was created for the 2 m horizontal co-planar sensor (H2) (Figure 2.5). The optimal fit for the power function parameters, α_H and β_H , from minimizing the sum of squared difference between predicted and observed depth to the argillic result in the following CRC function:

$$R_H = 11.006 \cdot e^{-6.016 \cdot \left(\frac{Z_{Clay}}{2}\right)} \quad \text{Equation 3.2}$$

In spite of Equation 3.2 having the best CRC fit, the predicted depths to the top of the argillic horizon correlated poorly with the observed depth with an $R^2 = 0.31$ (Figure 2.6). Overall, the response function (Equation 3.2) underestimates the depth to the top of the argillic horizon. The

CRC method was also applied at the U.S. Department of Energy's Savannah River Site, however, results showed that there was not enough variation in the depth to the argillic horizon for the method to be successful (see APPENDIX C).

In the multivariate approach, land-use was determined to be a significant variable (<0.0001) in predicting the depth to the argillic horizon; therefore, a model was created for each land use type (Table 2.2 and 2.3). Both land use models (Table 2.2 and 2.3) included other significant explanatory variables including slope and landscape position along with geophysical sensing data. For Watershed 3 and 4, soil borings and TPP data were originally pooled to predict depth-to-clay; however, the resulting regression including other landscape features was not a strong predictor ($R^2 = 0.28$). A significant prediction model using soil core data alone (not pooled soil core and TPP data), with other landscape features, for Watershed 3 and 4 ($n = 54$) was able to explain 66 % of the variation in the depth-to-argillic horizon (Table 2.2). When this model was applied to Watershed 3 and 4 separately the R^2 increased to 70 % in both watersheds. In the reference hillslopes, the pooled data with the soil boring and TPP data ($n = 86$) resulted in a model that only explained 24 % of the variability in the depth to the argillic horizon (Table 2.3). When the model was fit to each reference site separately it explained 65, 52, and 20 % of the variation for Reference 2, 4, and 9, respectively.

The final approach in analysis used the residuals from the above multivariate models to create site specific residual maps that were used in the regression kriging (RK) process to create predicted depth-to-argillic maps (Figures 2.7 and 2.8). The maps generated for the historically farmed sites had a larger range in depths (16 to 88 cm) relative to the reference hillslopes (23 to 39 cm) and showed shallower depths to the argillic horizon along the ridges and deeper in the floodplains. The maximum predicted depths using RK for historically farmed and reference sites

(88 and 39 cm, respectively) are similar to the average maximum observed depths of 87 ± 12 and 48 ± 12 cm, respectively (Table 2.1). A cross validation of the observed vs RK predicted depth to clay showed a slight increase in prediction accuracy compared to multivariate regression alone in reference hillslopes with an $R^2 = 0.27$ but a one percent decrease in prediction accuracy with an $R^2 = 0.69$ for previously farmed watersheds (Figure 2.9).

Discussion

Soil Sampling and Tile Push Probe

One objective for this research was to quantify the spatial variation in the depth to the argillic horizon within landscapes that had and had not been impacted by historical farming. Due to the strong correlation ($R^2 = 0.74$) between soil boring and TPP, the combined techniques allowed for an extensive investigation of the spatial variation in the depth to the argillic horizon along hillslope profiles. Direct measures indicated that historically farmed watersheds, although reforested since the 1930s, had a substantially redistributed soil in the mid-slope and toe-slope landscape position compared to reference hillslope with fairly consistent depths (Figure 2.4).

Previous studies investigating the depth to the argillic horizon in different land uses, in both the Coastal Plain and Piedmont have found comparable results to our study. For example, a study conducted on a first order forested upland watershed with similar soils (Tifton series) showed the depth to the argillic horizon in a historically farmed watershed increased towards the stream channel with approximately 50 cm of deposited soil, and undisturbed landscapes had an average depth to clay of 58 cm (Lowrance *et al.*, 1984). Several studies conducted in the Piedmont have shown 1 to 5 m of accumulated sediment present in floodplains of first to third order watersheds since the cotton farming era (Trimble, 1974; Jackson *et al.*, 2005b; Walter *et*

al., 2008; James, 2013). Our results support a lower slope deposition of farming era sediment, although this study found smaller thicknesses than previous estimations with an average of 40 cm more sediment in farmed toe-slopes compared to reference hillslopes (Table 2.1).

Analysis of Geophysical Sensing

A second objective was to determine the potential use of a geophysical sensing technique (EMI) as an accurate and efficient means to predict the depth-to-argillic horizon on upland, Piedmont landscapes. Clay soil contains a higher moisture content than sandier textures; therefore, the clay-rich subsoil should be distinguishable due to an expected higher electrical conductivity (Grasso *et al.*, 2005). We questioned if geophysical sensing would be able to describe at least 60 % of the variation in the depth to the argillic layer on these soils. Our results showed that electrical conductivity alone was not a strong predictor of the depth to the clay layer ($R^2 = 0.31$), although the strength of the prediction increased with the addition of other landscape features variables (*i.e.*, slope, and landscape position) ($R^2 = 0.69$; Figure 2.6 and 2.9).

Saey *et al.* (2011) found that a DUALEM-21S could predict the depth to the top of the argillic horizon with 95 % confidence using the CRC method on a homogenous loess capped argillic horizon in Belgium. When using the CRC method with our data, however, we predicted the clay horizon with 31 % confidence (Figure 2.6). This discrepancy could be explained by the heterogeneous nature of the Piedmont soils (Li *et al.*, 2010) and the absence of a distinct interface between top and subsoil, an important factor in the CRC method. Another possible explanation could be the effect of the geophysical data variability on the fit of the CRC model (*i.e.* power function parameters α_H and β_H). Sudduth *et al.* (2013) removed geophysical sensing measurements that had large (≥ 3.3 mS/m) standard deviations from the dataset, which proved

beneficial when fitting the response curve and predicting depth-to-clay; this approach was not implemented in this study. It may be possible that depth affects the prediction outcome as the response of the geophysical sensing device declines with depth (McNeill, 1980). For example, a previous study using linear regression between electrical conductivity and clay content was conducted on farmlands within the heterogeneous landscapes of the Tertiary hills of Southern Germany where surficial clay (i.e., <50) was predicted with 76 % confidence (Heil *et al.*, 2012). In comparison, in deep Vertisols on floodplains of New South Wales, Australia clay content was only 32 % correlated with inverse EMI data (Triantafilis *et al.* 2013a, b). Little work with geophysical sensing has been done in upland forested landscapes, although one study showed that percent clay in the top 30 cm correlated 73 % with geophysical sensing data on Mollisol hillslopes of Reynolds Mountain Experimental Watershed in Idaho (Robinson, 2008).

Predictions of clay content using geophysical sensing alone varied depending on soil type, depth of investigation, and land cover. However, it may be expected that some variation in spatial predictions can be improved with additional variables of landscape features (Hengl *et al.*, 2007). By adding landscape features easily extracted from DEM files to geophysical sensing outputs, our models showed an increase in prediction capability of depth to clay from 31 % (CRC method, Figure 2.6) to 69 % (RK method) in previously farmed watersheds (Figure 2.9). However, this was not observed in reference hillslopes, where a slight increase in prediction capability from 24 % (OLS method, Table 2.3) to 21 % (RK method, Figure 2.9) occurred. The landscape variables chosen (e.g., slope %) for this study were successful predictors within previously farmed watersheds and may reflect the overland flow and erosion process driving soil redistribution. However, in the reference hillslopes where there was a relatively constant depth to clay other soil properties such as underlying geology or porosity might be better predictors.

Correlating soil predictors with land use history was demonstrated in one study that used RK of pH with clay content to predicted previous land use (Braumoh et al., 2005). This study found that for predicting pH the variables of clay content, CEC, and soil color were important but only in the case of the soil being under native vegetation but not under cropland (Braumoh *et al.*, 2005). In the current study, RK did generally perform well in predicting the variation in depth-of-clay, which was larger in the historically farmed versus reference values. Additionally, the results of the RK predicted maximum depths to the argillic layer that were similar to those reported for each land use (Table 2.1).

Conclusion

We hypothesized that the mean depth to the argillic horizon would be shallower along the ridges and deeper throughout floodplains in the historically farmed landscapes than in the undisturbed reference landscapes due to poor land use practices in the watersheds (*i.e.*, tilling and the lack of erosion control). Our results provide support for a redistribution of soil and deposited sediment in lower slopes of previously farmed areas. This study, however, found thinner sediments in lower slopes than previous estimates. Direct depth-to-clay measurements are ideal, but they are labor intensive and result in point specific data rather than a continuous surface. Although geophysical sensing devices offer more spatial coverage, caution should be used when extrapolating to different landscapes, as statistical prediction models may not represent all land use types. Use of EMI with the addition of landscape feature characteristics (*i.e.*, slope, and landscape position), in this study in the upland Piedmont, appeared limited when predicting landscapes with uniform depth-to-clay (reference areas) but suggested geophysical

sensing is an efficient means of predicting larger variations in depth-to-clay such as those found on previously farmed sites.

References

Archer 2 GPS unit. Juniper System Inc., Logan, UT, U.S.A.

Braimoh, A. K., Stein, A., & Vlek, P. L. (2005). Identification and mapping of associations among soil variables. *Soil science*, *170*(2), 137-148.

Brecheisen, Z., Cook, C., & Harmon, M. (2015). US Forest Service Photograph from the Photographic Archive of the Calhoun Experimental Forest, <http://criticalzone.org/calhoun/data/dataset/4324/>.

Corwin, D., & Lesch, S. (2005). Apparent soil electrical conductivity measurements in agriculture. *Computers and electronics in agriculture*, *46*(1), 11-43.

Corwin, D., Lesch, S., Shouse, P., Soppe, R., & Ayars, J. (2003). Identifying soil properties that influence cotton yield using soil sampling directed by apparent soil electrical conductivity. *Agronomy Journal*, *95*(2), 352-364.

Coughlan, M. R., Nelson, D. R., Lonneman, M., & Block, A. E. (2017). Historical Land Use Dynamics in the Highly Degraded Landscape of the Calhoun Critical Zone Observatory. *Land*, *6*(2), 32.

De Benedetto, D., Castrignano, A., Sollitto, D., Modugno, F., Buttafuoco, G., & lo Papa, G. (2012). Integrating geophysical and geostatistical techniques to map the spatial variation of clay. *Geoderma*, *171*, 53-63.

Doolittle, J. A., & Brevik, E. C. (2014). The use of electromagnetic induction techniques in soils studies. *Geoderma*, *223*, 33-45.

Du, E., Jackson, C. R., Klaus, J., McDonnell, J. J., Griffiths, N. A., Williamson, M. F., Greco, J. L., & Bitew, M. (2016). Interflow dynamics on a low relief forested hillslope: Lots of fill, little spill. *Journal of Hydrology*, *534*, 648-658.

ESRI 2015. ArcGIS Desktop: Redlands, CA: Environmental Systems Research Institute.

- Galang, M., Markewitz, D., Morris, L., & Bussell, P. (2007). Land use change and gully erosion in the Piedmont region of South Carolina. *Journal of Soil and Water Conservation*, 62(3), 122-129.
- Gee, G. W., & Or, D. (2002). 2.4 Particle-size analysis. *Methods of Soil Analysis: Part 4 Physical Methods*(methodsofsoilan4), 255-293.
- GeoDa 1.8.14. Anselin, Luc, Ibnu Syabri and Youngihn Kho (2006). GeoDa: An Introduction to Spatial Data Analysis. *Geographical Analysis* 38 (1), 5-22.
- Golley, Frank B. (2004). Piedmont Geographic Region.
<http://www.georgiaencyclopedia.org/articles/geography-environment/piedmont-geographic-region>
- GoogleMaps. (2017). Sumter National Forest,
<https://www.google.com/maps/search/sumter+national+forest/@34.1570253,-83.4621966,7z/data=!3m1!4b1>.
- Grisso, R. D., Alley, M. M., Holshouser, D. L., & Thomason, W. E. (2009). Precision Farming Tools. Soil Electrical Conductivity. Available from: <http://pubs.ext.vt.edu/442/442-508/442-508.html>.
- Handheld Geographic Information Systems software (StarPal, Fort Collins, CO, U.S.A.)
- Heil, K., & Schmidhalter, U. (2012). Characterisation of soil texture variability using the apparent soil electrical conductivity at a highly variable site. *Computers & Geosciences*, 39, 98-110.
- Hengl, T., Heuvelink, G. B. M., & Rossiter, D. G. (2007). About regression-kriging: From equations to case studies. *Computers & Geosciences*, 33(10), 1301-1315.
doi:<http://dx.doi.org/10.1016/j.cageo.2007.05.001>
- Huang, C., Gascuel-Oudou, C., & Cros-Cayot, S. (2002). Hillslope topographic and hydrologic effects on overland flow and erosion. *CATENA*, 46(2-3), 177-188.
doi:[http://dx.doi.org/10.1016/S0341-8162\(01\)00165-5](http://dx.doi.org/10.1016/S0341-8162(01)00165-5)

- Jackson, C., Martin, J., Leigh, D., & West, L. (2005a). A southeastern piedmont watershed sediment budget: Evidence for a multi-millennial agricultural legacy. *Journal of Soil and Water Conservation*, 60(6), 298-310.
- Jackson, C. R., Martin, J. K., Leigh, D. S., & West, L. T. (2005b). A southeastern piedmont watershed sediment budget: Evidence for a multi-millennial agricultural legacy. *Journal of Soil and Water Conservation*, 60(6), 298-310.
- James, L. A. (2013). Legacy sediment: Definitions and processes of episodically produced anthropogenic sediment. *Anthropocene*, 2, 16-26.
doi:<http://dx.doi.org/10.1016/j.ancene.2013.04.001>
- Li, J., Mendoza, A., & Heine, P. (2010). Effects of land-use history on soil spatial heterogeneity of macro-and trace elements in the Southern Piedmont USA. *Geoderma*, 156(1), 60-73.
- Lowrance, R., Sharpe, J. K., & Sheridan, J. M. (1984). *Long term sediment deposition in the riparian zone of an agricultural watershed*. Retrieved from United States: <http://proxy-remote.galib.uga.edu/login?url=http://search.ebscohost.com/login.aspx?direct=true&db=geh&AN=1988-069057&site=eds-live>
- McNeill, J. (1980). Electromagnetic terrain conductivity measurement at low induction numbers. Geonics Technical Notes. TN - 6. 15 pp: Geonics Limited Ontario, Canada
- Metz, L. J. (1958). The Calhoun Experimental Forest. US Forest Service Southeastern Forest Experiment Station. Available online:
https://www.srs.fs.usda.gov/pubs/misc/metz_calhoun.pdf
- NCALM. (2016). National Center for Airborne Laser Mapping (NCALM), Calhoun Critical Zone Observatory 2016 Leaf Off LiDAR Survey, funded by National Science Foundation (EAR-1339015, EAR-1331846).
<http://opentopo.sdsc.edu/datasetMetadata?otCollectionID=OT.072016.26917.2>.
- PC-Progress. HYDRUS 2-D. Pruge, Czech Republic. URL: <https://www.pc-progress.com/en/default.aspx>

Rhoades, J., Manteghi, N., Shouse, P., & Alves, W. (1989). Soil electrical conductivity and soil salinity: New formulations and calibrations. *Soil Science Society of America Journal*, 53(2), 433-439.

Richter, D. D., Bacon, A. R., Billings, S. A., Binkley, D., Buford, M., Callahan, M. A., Curry, A. E., Fimmen, R. L., Grandy, A. S., Heine, P. R., Hofmockel, M., Jacks, J. A., LeMaster, E., Li, J., Markewitz, D., Mobley, M. L., Morrison, M. W., Strickland, M. S., Waldrop, T., and Wells, C. G., (2015). *Evolution of soil, ecosystem, and critical zone research at the USDA FS Calhoun Experimental Forest* (Vol. 18).

Richter, D. D., & Markewitz, D. (2001). *Understanding soil change: soil sustainability over millennia, centuries, and decades*: Cambridge University Press.

Richter, D. D., Markewitz, D., Heine, P. R., Jin, V., Raikes, J., Tian, K., & Wells, C. G. (2000). Legacies of agriculture and forest regrowth in the nitrogen of old-field soils. *Forest Ecology and Management*, 138(1), 233-248.

Richter, D. D., Markewitz, D., Wells, C., Allen, H., April, R., Heine, P., & Urrego, B. (1994). Soil chemical change during three decades in an old-field loblolly pine (*Pinus taeda* L.) ecosystem. *Ecology*, 75(5), 1463-1473.

Robinson, D. A., Abdu, H., Jones, S. B., Seyfried, M., Lebron, I., & Knight, R. (2008). Eco-geophysical imaging of watershed-scale soil patterns links with plant community spatial patterns. *Vadose Zone Journal*, 7(4), 1132-1138.

Ryland, R. (2017). "CZO Dataset: Calhoun CZO - Soil Texture - Argillic Horizon (2016 - 2017)". <http://criticalzone.org/calhoun/data/dataset/5982/>.

Saey, T., Van Meirvenne, M., De Smedt, P., Cockx, L., Meerschman, E., Islam, M. M., & Meeuws, F. (2011). Mapping depth-to-clay using fitted multiple depth response curves of a proximal EMI sensor. *Geoderma*, 162(1), 151-158.

Shanahan, P. W., Binley, A., Whalley, W. R., & Watts, C. W. (2015). The use of electromagnetic induction to monitor changes in soil moisture profiles beneath different wheat genotypes. *Soil Science Society of America Journal*, 79(2), 459-466.

- Sudduth, K., Drummond, S., & Kitchen, N. (2001). Accuracy issues in electromagnetic induction sensing of soil electrical conductivity for precision agriculture. *Computers and electronics in agriculture*, 31(3), 239-264.
- Sudduth, K., Kitchen, N., Bollero, G., Bullock, D., & Wiebold, W. (2003). Comparison of electromagnetic induction and direct sensing of soil electrical conductivity. *Agronomy Journal*, 95(3), 472-482.
- Sudduth, K. A., Kitchen, N. R., Myers, D. B., & Drummond, S. T. (2010). Mapping depth to argillic soil horizons using apparent electrical conductivity. *Journal of Environmental & Engineering Geophysics*, 15(3), 135-146.
- Sudduth, K. A., Myers, D. B., Kitchen, N. R., & Drummond, S. T. (2013). Modeling soil electrical conductivity–depth relationships with data from proximal and penetrating ECa sensors. *Geoderma*, 199, 12-21.
- Triantafilis, J., Terhune, C., & Santos, F. M. (2013a). An inversion approach to generate electromagnetic conductivity images from signal data. *Environmental modelling & software*, 43, 88-95.
- Triantafilis, J., & Santos, F. M. (2013b). Electromagnetic conductivity imaging (EMCI) of soil using a DUALEM-421 and inversion modelling software (EM4Soil). *Geoderma*, 211, 28-38.
- Trimble, S. W. (1974). Man-induced soil erosion on the southern Piedmont. *Soil Conserv. Soc. Am., Ankeny, Iowa*, 1700-1970.
- Walter, R. C., & Merritts, D. J. (2008). Natural streams and the legacy of water-powered mills. *Science*, 319(5861), 299-304.
- Wegmann, K. W., Lewis, R. Q., & Hunt, M. C. (2012). Historic mill ponds and piedmont stream water quality: Making the connection near Raleigh, North Carolina. *Field Guides*, 29, 93-121.
- Weller, U., Zipprich, M., Sommer, M., Castell, W. Z., & , & Wehrhan, M. (2007). Mapping clay content across boundaries at the landscape scale with electromagnetic induction. *Soil Science Society of America Journal*, 71(6), 1740-1747.

White, M. L., Shaw, J. N., Raper, R. L., Rodekohr, D., & Wood, C. W. (2012). A multivariate approach for high-resolution soil survey development. *Soil science*, 177(5), 345-354.

Worsham, L., Markewitz, D., Nibbelink, N. P., & West, L. T. (2012). A comparison of three field sampling methods to estimate soil carbon content. *Forest Science*, 58(5), 513-522.

Table 2.1: Mean depth to the argillic horizon as measured by tile push probe and observed from field soil cores (cm) for historically farmed and reference sites by landscape position in the Calhoun Critical Zone Observatory, SC. Data is represented as an average \pm standard deviation (SD).

Landscape Position	Historically Farmed Watersheds		Reference Hillslopes	
	Push Probe N = 223 (cm \pm SD)	Soil Cores N = 82 * (cm \pm SD)	Push Probe N = 52 (cm \pm SD)	Soil Cores N = 8 ** (cm \pm SD)
Ridge	26 \pm 2.36	30 \pm 3.09	34 \pm 1.78	45 \pm 12.78
Shoulder	33 \pm 2.18	40 \pm 3.54	30 \pm 1.23	.
Mid-slope	44 \pm 3.24	43 \pm 5.46	30 \pm 1.03	37 \pm 1.67
Foot-slope	49 \pm 4.42	71 \pm 7.34	30 \pm 0.86	.
Toe-slope	59 \pm 7.50	87 \pm 12.38	34 \pm 5.91	48 \pm 12.50

* 19 additional soil cores had no evidence of an argillic horizon to 200 cm.

** One additional core had no evidence of an argillic horizon to 200 cm.

Table 2.2: Ordinary least squared regression used to predict the depth-to-clay (from soil core data) for two historically farmed landscapes (Watershed 3 and 4) within the Calhoun Critical Zone Observatory, SC. Variables for the model included: slope, landscape position and geophysical output data (EMI), with the addition of site specific residuals for regression kriging purposes ($R^2 = 0.66$).

Variable	Coefficient	Stand. Error
Constant	42.5371	8.50441
Slope (%)	1.10412	0.232
Ridge	-29.7855	6.76652
Shoulder	-26.2071	6.50691
Mid Slope	-16.8688	6.13057
(H2-P2) + 6	1.75754	1.31129
Residual		

Table 2.3: Ordinary least squared regression used to predict the depth-to-clay (using soil core and tile push probe data) for three reference hillslopes (Reference 2, 4, and 9) in the Calhoun Critical Zone Observatory, SC. Variables for the model included: slope, landscape position, geophysical output data (EMI), with the addition of site specific residuals for regression kriging purposes ($R^2 = 0.24$).

Variable	Coefficient	Stand. Error
Constant	33.3001	4.42821
Slope (%)	-0.224102	0.108637
H2	-1.4439	0.438051
(H2-H1) +10	-0.625756	0.401208
Ridge	9.86033	3.10772
Shoulder	5.88184	3.16284
Mid Slope	7.5026	2.93936
Foot Slope	7.48241	3.06812
Residual		

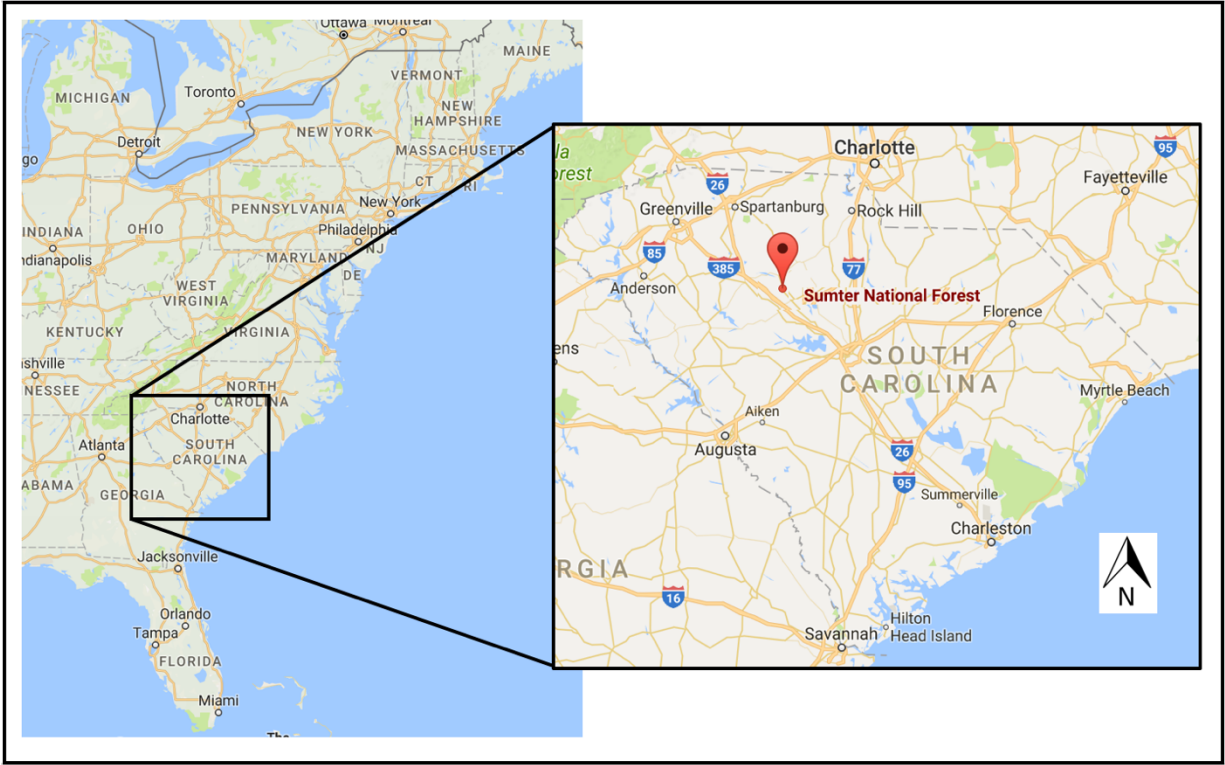


Figure 2.1: The Calhoun Critical Zone Observatory research site located within the Sumter National Forest, South Carolina USA (GoogleMaps, 2017).

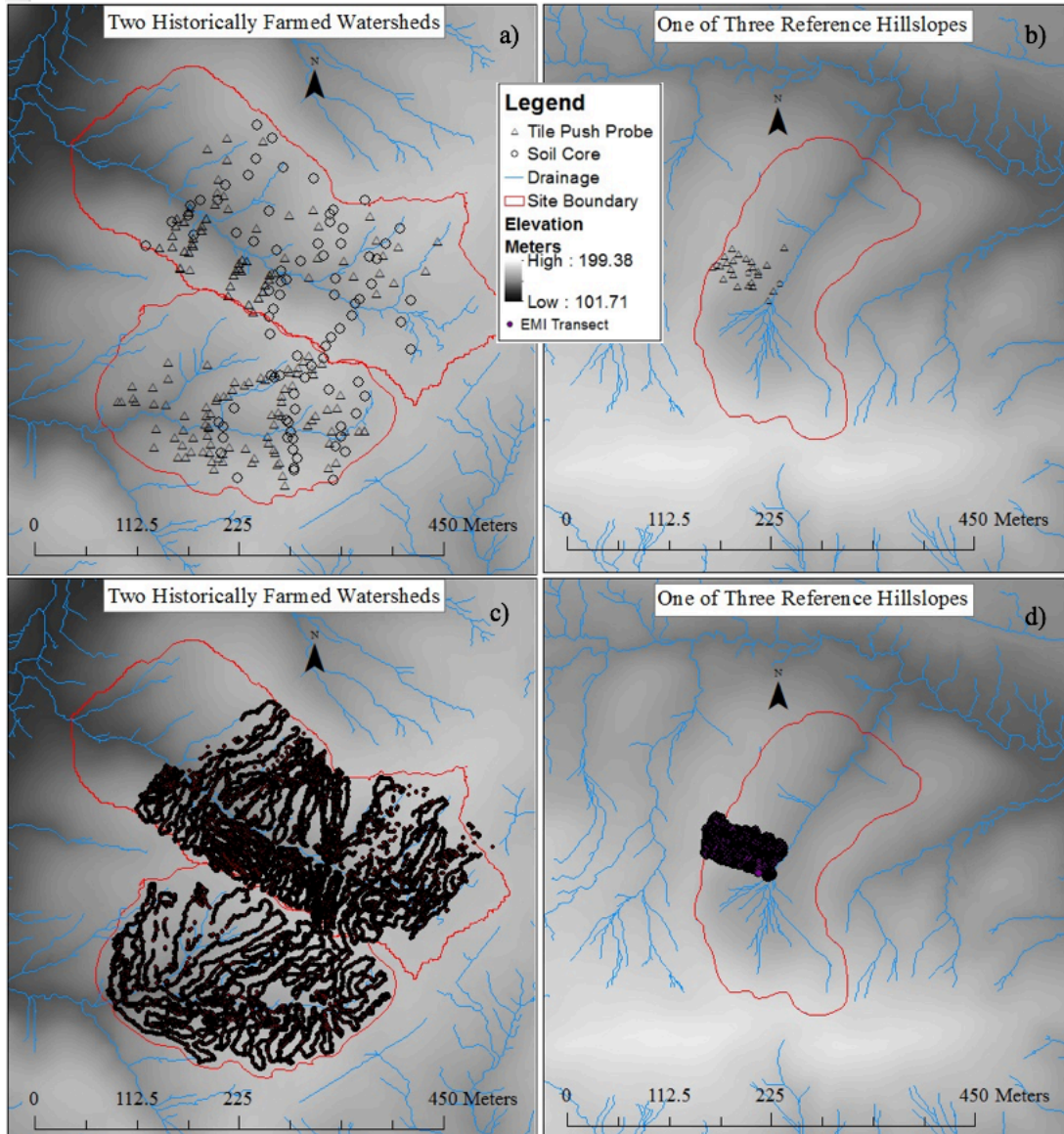


Figure 2.2: Soil core and tile push probe locations as well as a digital elevation model (DEM) of a) highly eroded, historically farmed watershed showing steep topographical relief and gully, b) DEM for one of three reference hillslopes (Reference 4) with smooth topographical relief, c) geophysical sensing (EMI) transects in historically farmed and d) reference landscapes. Approximately 30,000 geophysical sensing observation points for historically farmed and 7,000 for reference hillslopes are presented.

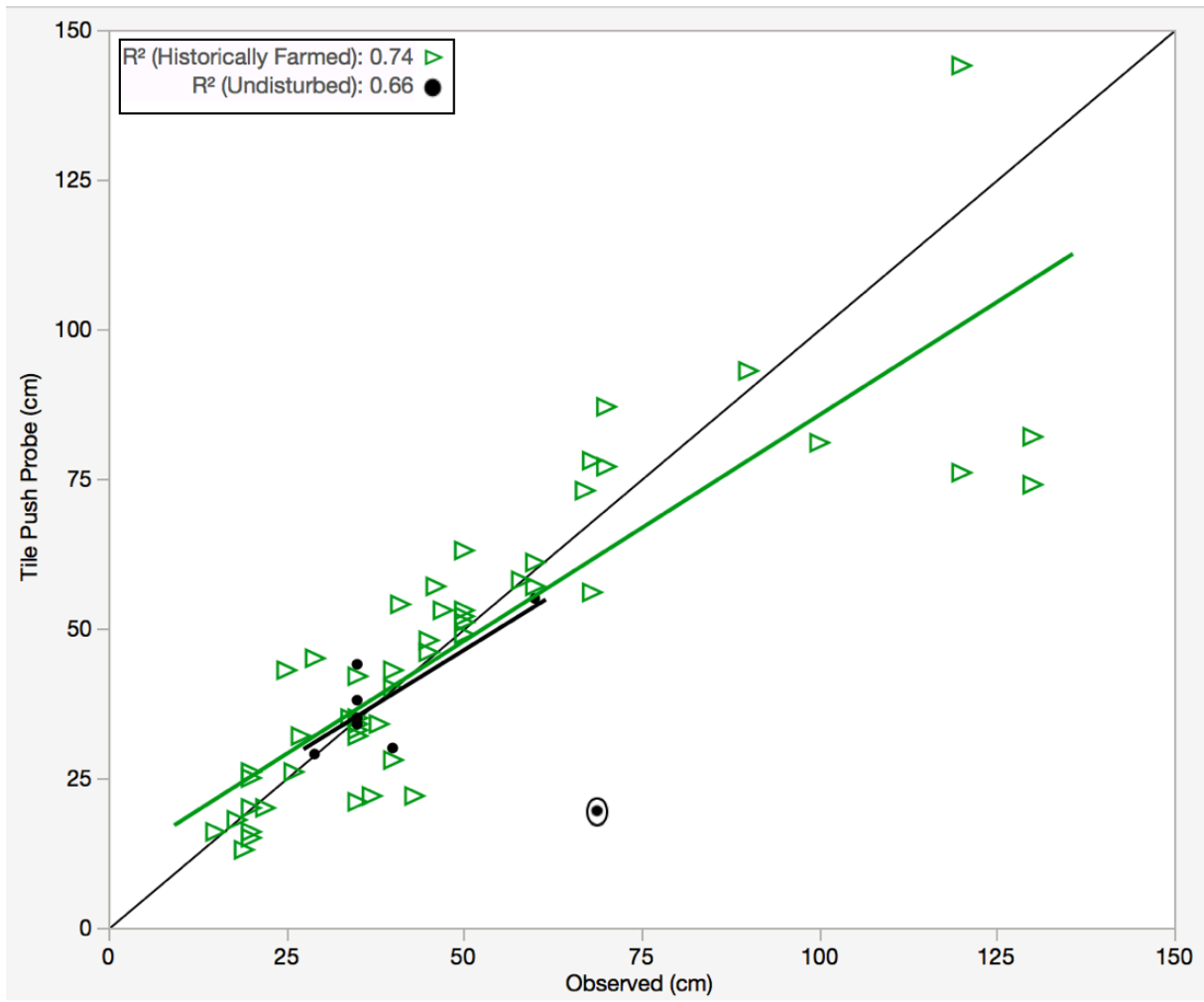


Figure 2.3: Comparison of the depth to the argillic horizon measured by tile push probe (y-axis) and soil auguring (x-axis) for historically farmed (triangle) $R^2 = 0.74$, and reference hillslopes (circle) $R^2 = 0.66$ (the circled measurement was removed before computing correlation). Lines indicate 1:1 correlation.

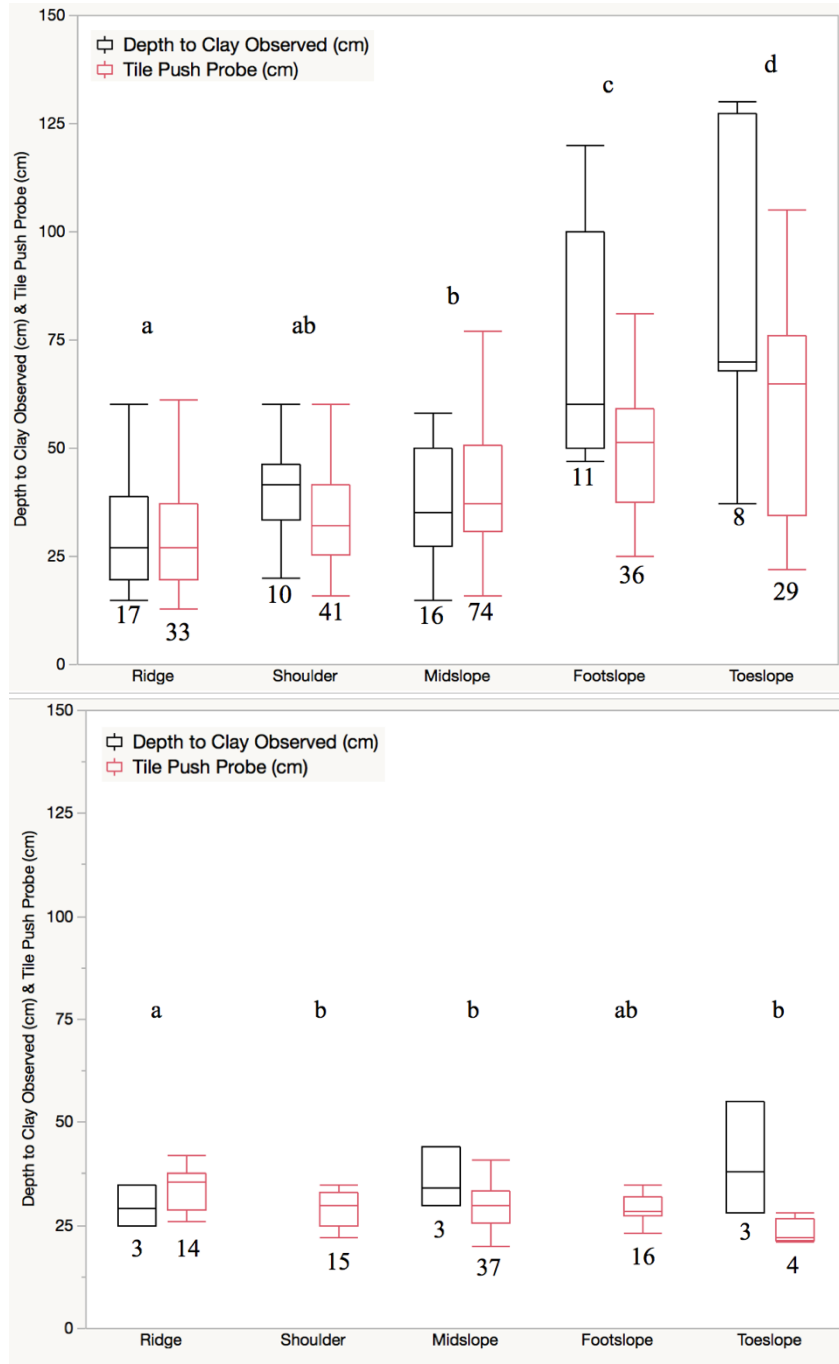


Figure 2.4: Depth to the argillic horizon along hillslope profile as observed by soil boring (black) and tile push probe (red) in Calhoun Critical Zone Observatory, SC for historically farmed (top, n = 275) and reference landscapes (bottom, n = 122). Sample size (n) for each sample at each landscape position is located below each boxplot. The flat ridge top is preceded by the convex shoulder in the upper portions of the landscapes, and the concave foot-slope is preceded by a flat toe-slope in the lower portions of the landscapes.

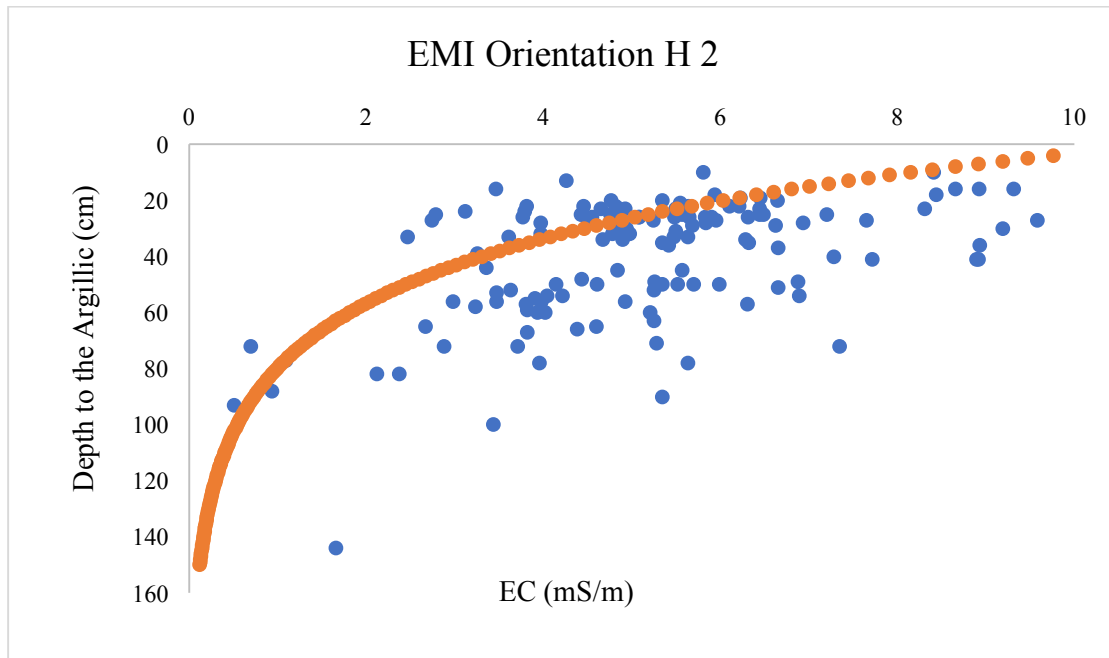


Figure 2.5: Cumulative depth response curve (orange) for EMI sensor orientation H2. Blue dots represent extracted EMI values from 2015 measurements at points also measured by soil auger or tile push probe. Sampling was from the historically farmed Watershed 3 within the Calhoun Critical Zone Observatory, SC.

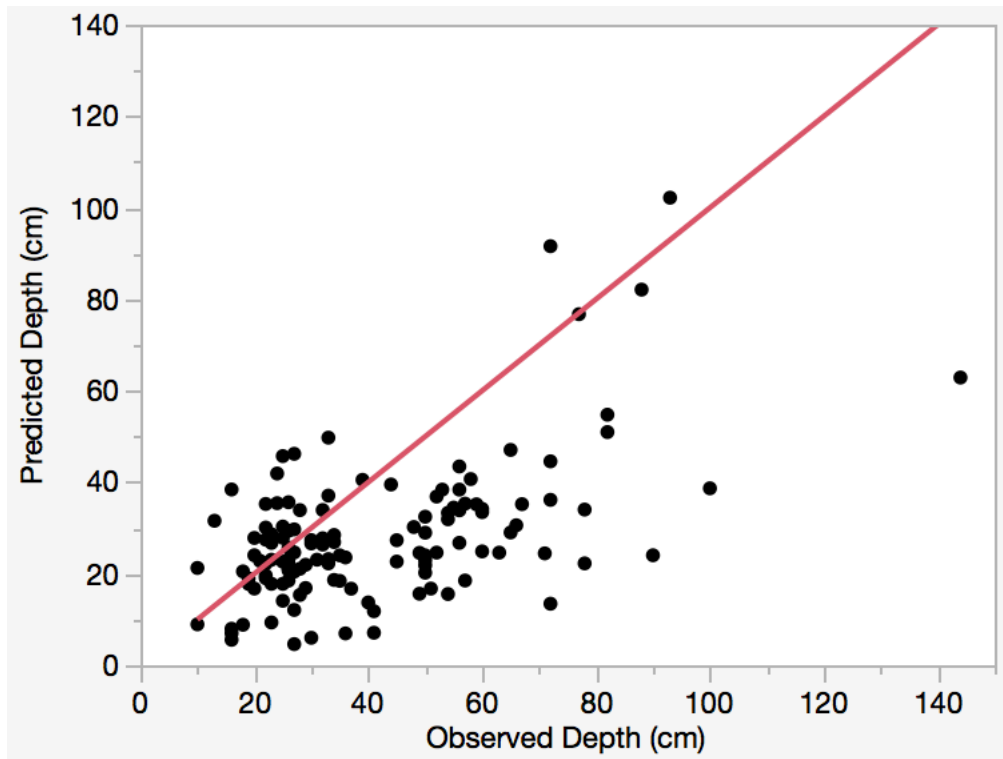


Figure 2.6: Comparison of the depth to the argillic horizon predicted by cumulative response curve for EMI sensor orientation H2 (y-axis) and observed depth from soil auguring (x-axis) for previously farmed watershed 3. Line indicates 1:1 correlation, best fit line $R^2 = 0.31$.

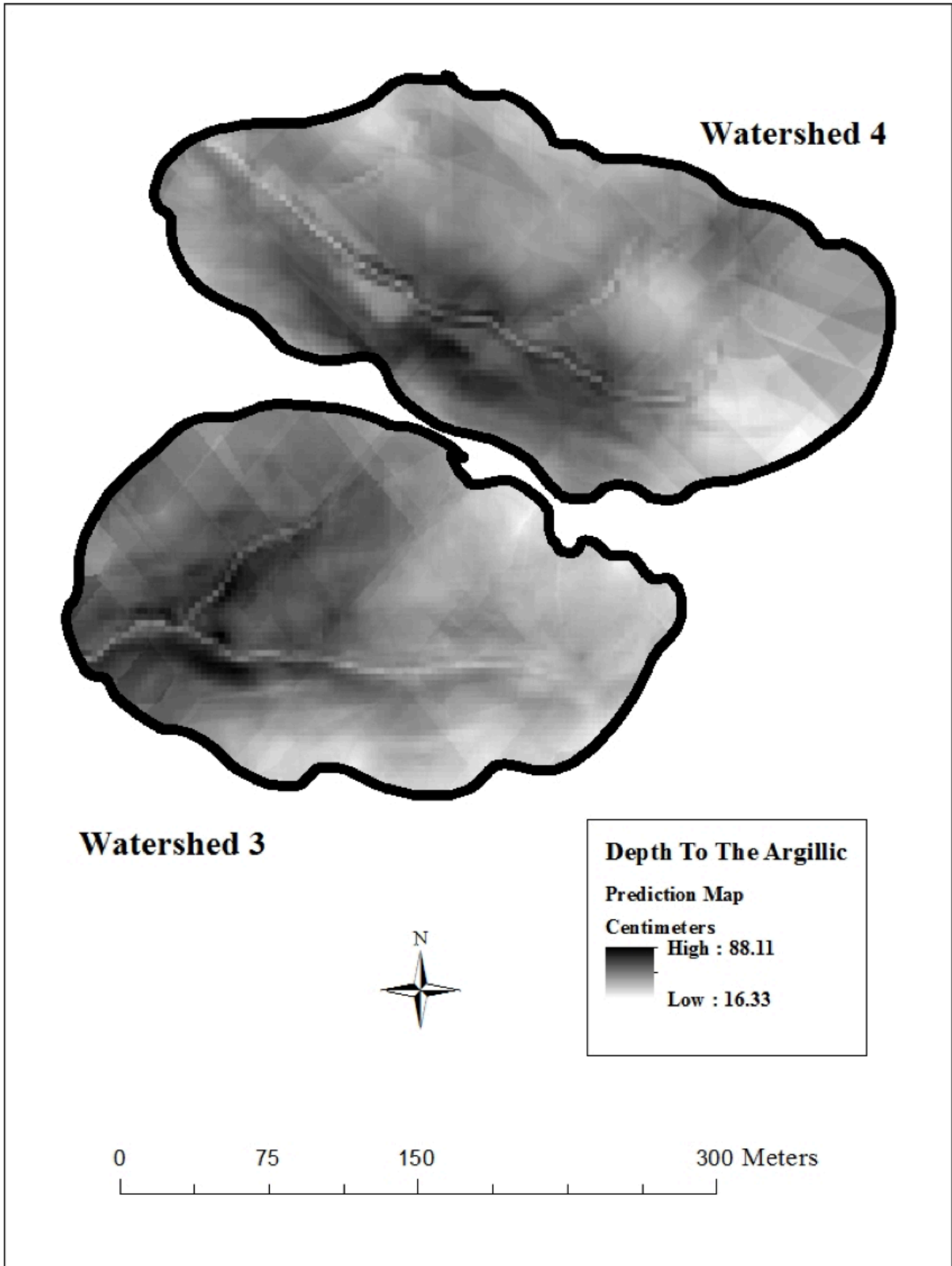


Figure 2.7: Predicted depth to the argillic horizon maps created using regression kriging for previously farmed watersheds in the CCZO, SC.

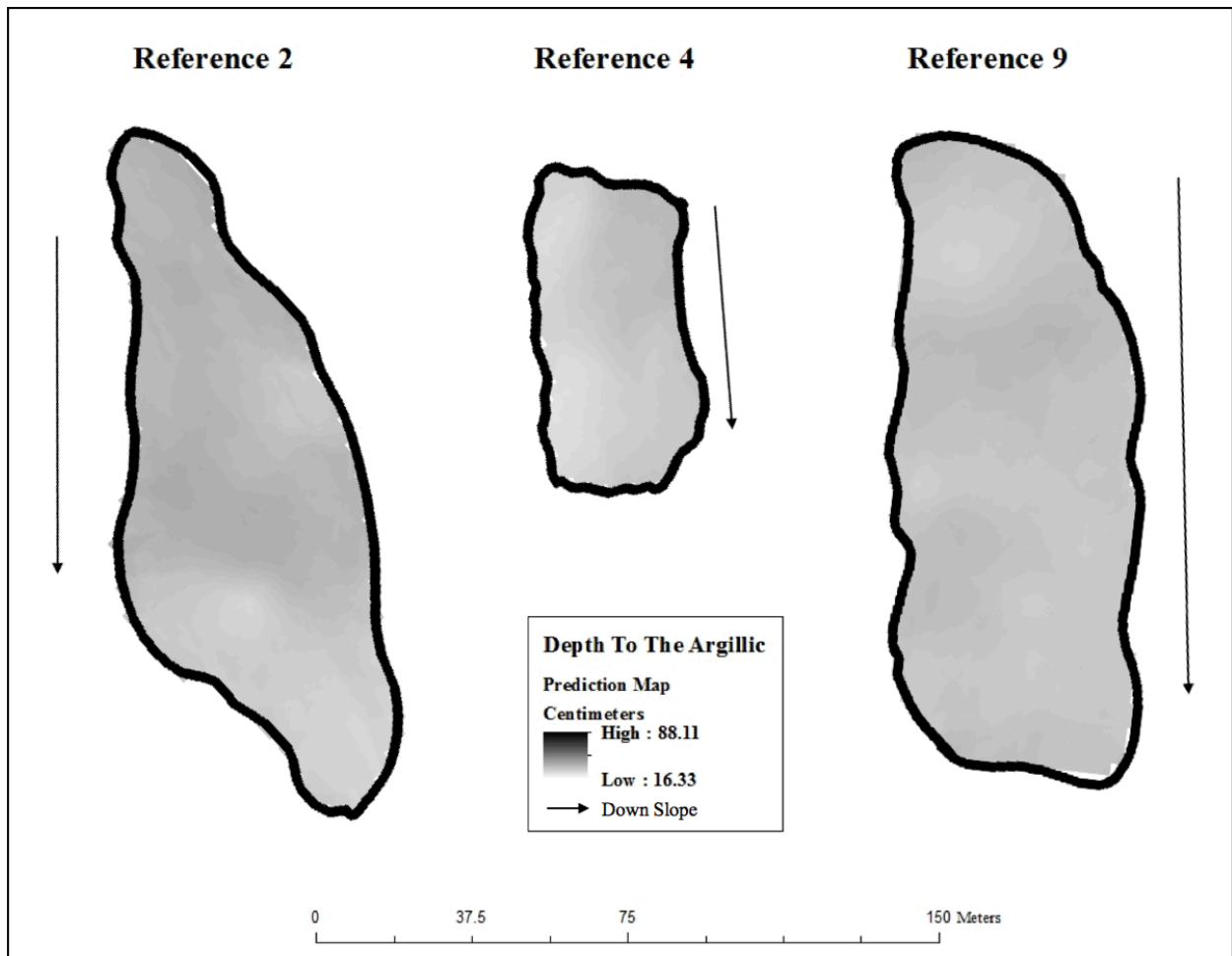


Figure 2.8: Predicted depth to the argillic horizon maps created using regression kriging for three reference hillslopes in the CCZO, SC. Arrows point towards downslope.

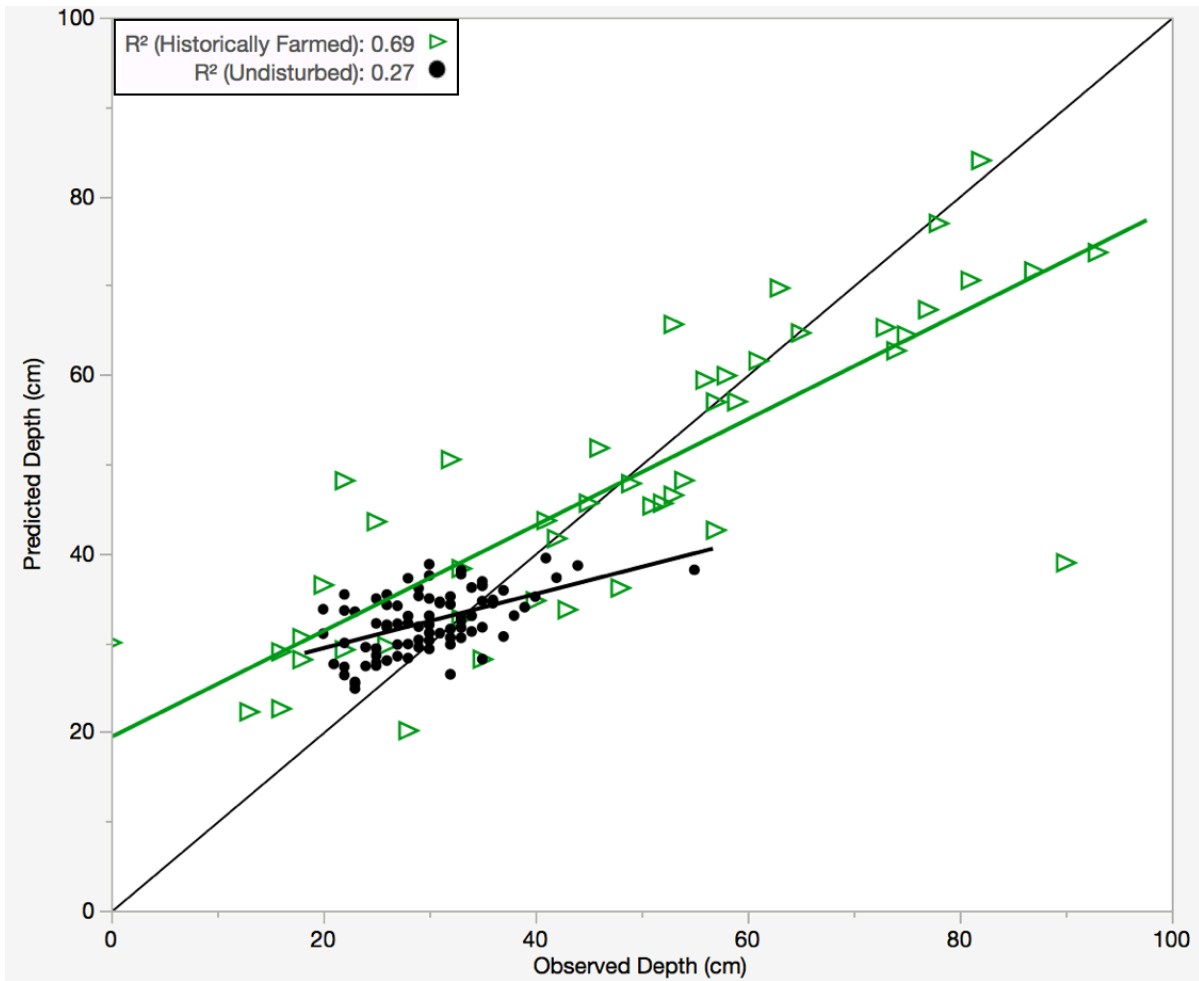


Figure 2.9: Comparison of the depth to the argillic horizon predicted by regression kriging (y-axis) and observed depth from soil auguring (x-axis) for historically farmed (triangle) $R^2 = 0.69$ and reference hillslopes (circles) $R^2 = 0.27$. Lines indicate 1:1 correlation.

CHAPTER 3

EVALUATION OF ALTERED DEPTHS TO THE ARGILLIC HORIZON DUE TO EROSION: WHAT IMPACTS ON HILLSLOPE INTERFLOW?

¹ Ryland R.C., D. Markewitz, and A. Thompson. 2017. To be submitted to Journal of Hydrology.

Abstract

Numerical models of hillslope hydrology often use characteristics from soil classification maps to parameterize subsurface hydrologic flow paths. These soil maps, however, may lack sufficient spatial detail and may not accurately represent landscapes that have been eroded from historical farming. Therefore, a spatially explicit model of eroded landscapes, particularly in the Piedmont region of the southeast USA, could be valuable. Hillslope hydrology of the Piedmont typically involves an argillic horizon with low permeability causing high lateral flow in periods of high precipitation. In hillslope models this layer of low permeability is generally parallel to the soil surface. Highly eroded landscapes, such as those within South Carolina's Calhoun Critical Zone Observatory, have had a redistribution of surface soil to lower landscape positions altering the depth to the low permeable layer and possibly altering patterns of interflow. This study aimed to understand variations of topsoil thickness and depth to the argillic horizon on hillslope interflow. Using a two-dimensional simulation model parameterized with site specific measurements (i.e., precipitation, K_{sat} , etc) topsoil thickness and depth to the argillic were altered to compare simulation outputs with uniform and non-uniform thicknesses. Results indicated that the non-uniform depth-to-clay model had lower water content in the topsoil (by 9.4%) and limiting layer (water content ranged from 25.3 to 37.9 %) but increased water storage (4.6%) compared to uniform depth-to-clay, over the two-year simulation period. An increase in topsoil depth in lower slope positions from historic erosion may have altered lower slope water storage and the hydrologic gradient driving interflow.

Introduction

Historical agricultural practices in the Piedmont region of the southeastern USA led to accelerated erosion throughout the region from the early 1800s to the 1930s (Trimble, 1974). These practices degraded soil quality, altering surface hydrologic processes across the landscapes by limiting infiltration and leading to overland flow and erosion (Huang *et al.*, 2002). Hillslope hydrology of the Piedmont is strongly influenced by an argillic horizon with low permeability, which causes high lateral flow (on top of or within the argillic horizon) in periods of high precipitation (Dreps, 2011). Accelerated erosion in this region has resulted in soil redistribution from upper to lower landscape positions (Gabbard *et al.*, 1998), compared to landscapes with minimal agricultural disturbance that tend to have a nearly consistent depth of topsoil (Figure 2.4). Such redistribution is rarely accounted for in efforts to model hillslope and watershed hydrology in this region.

Numerical models of hillslope and watershed hydrology typically have estimated topsoil thickness either from soil classification maps (Dialynas *et al.*, 2016) or digital elevation models (Quinn *et al.*, 1991; Paniconi *et al.*, 1993), or they have approximated a topsoil thickness parallel to the soil surface (O'loughlin, 1981; Jackson *et al.*, 2014). To quantify hillslope interflow, these approximations may lack sufficient spatial detail and may not accurately represent non-uniform subsoil topographies where different zones of interflow occur on low permeability, argillic horizons (Du *et al.*, 2016). Studies have shown that non-parallel topographies of hydraulically limiting subsoil can cause variation in water content along the hillslope (*i.e.* perched water table) as opposed to uniform topsoil thicknesses, which creates infrequent interflow events (Chaplot *et al.*, 2003; Ali *et al.*, 2011; Du *et al.*, 2016). Therefore, a spatially explicit hillslope model

containing a non-uniform topsoil thickness could create zones of interflow that are different than current estimates that use uniform topsoil thickness to argillic horizons.

The objective of this research was twofold. First, we quantified differences in field saturated hydraulic conductivity across Piedmont landscapes with evidence of historic farming and erosion (non-uniform depth to clay) relative to others that did not show evidence of farming (uniform depth-to-clay). Second, these measurements as well as other site characteristics (*i.e.* depth-to-argillic, climate data) were used to parameterize two HYDRUS-2D computational models, one for each depth-to-clay scenario (uniform and non-uniform). A comparison of the hillslope hydrology between uniform and non-uniform models was conducted with particle tracking (to visualize interflow pathways), variations in water content, and a water budget at the end of a two-year simulation to determine net soil water storage. We hypothesized that interflow would be higher in the uniform depth-to-clay hillslope and soil water storage would be lower due to the thinner topsoil thickness at the toe-slope, compared to the non-uniform depth-to-clay model.

Methods

Study Site

The Calhoun Critical Zone Observatory (CCZO) is based in the USDA Forest Service Sumter National Forest in the South Carolina Piedmont and incorporates the historical Calhoun Experimental Forest (Figure 3.1). Cultivation of cotton, corn, wheat, and other crops led to significant soil erosion throughout the Piedmont starting circa 1800 and continued into the early twentieth century when the land was abandoned from agriculture (Trimble, 1974; Richter *et al.*, 2001). The mean annual precipitation is approximately 1260 mm, and the mean annual

temperature is approximately 17 °C. Elevation ranges from 113 to 196 m above sea level. Soils in this area are mostly highly weathered acidic Ultisol and Inceptisol soils (Richter *et al.*, 2015).

The depth-to-argillic horizon and hydraulic conductivity measurements for this study were conducted at six locations within the CCZO; three previously farmed watersheds that were abandoned in the 1940s and three hillslopes undisturbed by agriculture. Histories of land use were determined via aerial photograph of the CCZO taken near the time of abandonment of agriculture clearings as well as forested hardwoods that can be identified in these 1933 aerial photos (Brecheisen *et al.*, 2015).

The average north facing slope for the two of the historically farmed watersheds (watershed 3 and 4) was steeper at 41.0 percent slope than the average south facing slope at 24.1 percent slope. The length of the slopes, for the two historically farmed watersheds, also differed depending on the direction the slopes faced. The north facing slopes on average were 50.1 m, and the south facing were on average 91.8 m.

Hydrologic Model Inputs and Structure

Two hillslope model formulations were designed to simulate daily changes in the vertical and horizontal distribution of soil water for 1) uniform topsoil thickness (hillslopes undisturbed by agriculture) and 2) non-uniform topsoil thickness (historically farmed hillslopes) using HYDRUS 2D version 2.05 (PC-Progress, Prague, Czech Republic). These formulations incorporated the site-specific soil characteristics of hydraulic conductivity, depth to the argillic horizon, and texture. Values for additional variables: precipitation, evaporation, rooting depth, slope and root water uptake, were applied from previous studies conducted either in the CCZO or the Piedmont region. All other variables (*i.e.* water retention curve parameters, initial water

content conditions, and boundary conditions) were estimated by using databases within the HYDRUS software. The hillslope formulations consisted of a soil system that ranged in depth from 5.0 m at the ridgeline to 2.0 m at the toe-slope seepage face. The system contained three soil horizons: a sandy topsoil, a clay-rich, low permeability argillic layer, and a sandy sub-limiting layer. The only differences among the hillslope models was topsoil thickness. Topsoil in the non-uniform model was the same depth as the uniform model at the ridge but increased in depth at the foot-slope; the uniform model had a consistent topsoil thickness for the entire hillslope. The effect of topsoil thickness on soil water storage was estimated through the water budget, and interflow was visualized via particle tracking with interflow across the seepage face again estimated by changes in water content.

Originally, the two hillslope formulations consisted of a percent slope and slope length (100 m) similar to those found in the study site, however, the large formulations were limited as the run time was several hours long often failing before the simulation period was over. Therefore, smaller hillslope formulations were developed with shorter slope lengths (16.5 m) to produce shorter run times.

Model Description and Parameterization

HYDRUS-2D/3D is a computational computer program that simulates water transport (Šimůnek *et al.*, 2016). The program numerically solves the Richards (1931) equation for saturated and unsaturated water flow and can model varying pressure head boundary conditions. Water flow is calculated using a finite element mesh which creates a triangular mesh network of nodes throughout the 2D hillslope modeling space.

Two hillslope models with near identical parameters, except for the thickness of topsoil, were developed. Both hillslope models simulate daily precipitation and evapotranspiration for a period of 270 days (initialization period) from March 1958 to December 1958 and an additional two years of simulation from December 1958 to December 1960 (total of 1008 days). These two years (1959 and 1960) were chosen because of the large amount of precipitation (average precipitation for 1959 and 1960 are 156.96 cm), which was expected to cause more interflow and storage (Figure 3.2). Rainfall data were extracted from measurements originally collected from 1949 – 1962 (average rainfall for 1949 – 1962 was 109.47 cm) by scientists of the USDA-FS Southern Experiment Station (Wang *et al.*, 2015). Daily evapotranspiration data from 1958 to 1960 were obtained from the NOAA National Center of Environmental Information online data ordering service (NCEI, 2016) for Station: Union 8S, SC US GHCND: USC00388786 (Elevation 480 ft. Latitude 34.605 °. Longitude 81.663 °).

Precipitation and evapotranspiration interact with the hillslope model via the atmospheric boundary condition along the soil surface. Infiltration is treated as a negative flux across the atmospheric boundary into the hillslope and evaporation a positive flux across the boundary out of the hillslope. The groundwater outlet at the bottom of the hillslope along the bank was represented as a drainage face (seepage face boundary; Figure 3.3). Drainage from the seepage face occurs when the water content of the soil is greater than field capacity. The pressure head along the seepage face is equal to zero for the saturated part of the seepage face and the outflow is equal to zero for the unsaturated portion of the seepage boundary. A no flux boundary condition was used for both the bottom of the modeled space (*i.e.*, bedrock) and below the ridgeline at the upper hillslope (*i.e.*, the ridgeline; Figure 3.3).

Soil texture and horizon distribution along the hillslope within both model spaces were based on previous data reported (Figure 2.4) and are similar in profile to the Ultisols found at the study site with a sandy capped argillic layer. Only the thickness of the topsoil horizon was changed depending on the model. The distribution of topsoil thickness is based on the average depth of topsoil observed in the field so is not an even re-distribution of the same volume of topsoil from the uniform to the non-uniform model. The uniform model had a consistent sandy loam topsoil thickness of 40 cm while in the non-uniform model the sandy loam topsoil ranged from 40 cm at the ridge to 50 cm at the mid-slope and 80 cm at the lower slope. Both models had a 60 cm thick clay impeding layer directly under the topsoil, and a sandy loam subsoil which filled the remaining modeled space (Figure 3.4).

Water retention parameters for both hillslope models are shown in Table 3.1. Saturated hydraulic conductivity (K_{sat}) was measured on site by a compact constant head permeameter (Amoozegar, 1989). The residual volumetric water content (θ_r), saturated volumetric water content (θ_s), and the water retention functions α and n were estimated using the Neural Network Prediction option (Schaap *et al.*, 1998) within the soil hydraulic parameters of HYDRUS 2D. This option uses the Rosetta Model (Schaap *et al.*, 2001) to predict Van Genuchten's water retention parameters (Van Genuchten, 1987) from textural information.

$$\theta(h) = \frac{\theta_s - \theta_r}{[1 + (-\alpha h)^n]^m} + \theta_r \quad \text{Equation 4.1}$$

Where α (cm^{-3}), m (dimensionless), and n (dimensionless) are fitted parameters, $\theta(h)$ is the volumetric water content ($\text{cm}^3 \text{ cm}^{-3}$), θ_s is the saturated volumetric water content ($\text{cm}^3 \text{ cm}^{-3}$), and θ_r is the residual volumetric water content ($\text{cm}^3 \text{ cm}^{-3}$). Initial water content of the hillslope was

set to field capacity for the entire hillslope domain. Field capacity values changed depending on the soil texture and were based on databases within the HYDRUS 2D software. These values were -100.91 cm for sandy loam topsoil, -181.783 cm for the clay impeding layer, and -143.698 for a sandy loam subsoil. This condition was used at the beginning of the model simulation of 1008 days.

The root uptake parameters were estimated within the HYDRUS 2D software, where root water uptake is modeled as a function of soil water pressure head (Feddes *et al.*, 1978).

$$S(h) = \alpha(h)S_{\max} \quad \text{Equation 4.2}$$

The root water uptake $S(h)$ is the volume of water removed from a volume of soil per unit time (T^{-1}), α is the stress response function of pressure head (-), and S_{\max} is the maximum potential water uptake rate (T^{-1}). There are four pressure heads used within the model: h_1 , h_2 , h_3 , and h_4 . If the pressure head is less than h_4 (wilting point) or greater than h_1 (saturation) then the root water uptake is equal to zero. Plant available water was optimal between h_2 and h_3 . Values used for root water uptake parameters were $h_1 = -10$ cm, $h_2 = -25$ cm, $h_3 = -300$ cm, $h_4 = -15000$ cm and $S_{\max} = 0.5$ cm d^{-1} (estimated within HYDRUS 2D). The root distribution (Figure 3.5) was set as an exponential decay gradient from the soil surface to the bottom of the modeled space using a root biomass distribution for a pine plantation located within the southeastern Piedmont (Qi, 2016).

Model Comparison

To understand the effect of topsoil thickness on interflow, a comparison of the uniform and non-uniform models was conducted using three different measures: particle tracking, water content, and annual water budget. First, the location and movement of five particles located within the topsoil along the atmospheric boundary were overlaid on the simulation run. The flow paths created by this particle tracking assist in visually identifying any lateral movement within the top two soil horizons. Second, water content (θ), detected by an observation node at the seepage face boundary, was measured at one location within each soil horizon to estimate water flux contributed by that soil horizon over the simulation run. Variations in water content of the hillslope profiles was also compared at the end of the simulation run. Third, an annual water budget for each topsoil thickness scenario was calculated from January to December for 1959 and 1960. The water budget was conducted to assess the effect of topsoil thickness on hillslope soil water storage.

$$\Delta S = P - RWU - Seepage \quad \text{Equation 4.3}$$

Where ΔS was the change in soil water storage (cm), P was precipitation (*note*: all precipitation infiltrates into the soil; cm), RWU was root water uptake (cm), and *Seepage* was the flux of ground water from the hillslope out the seepage face boundary (cm). Soil water storage in cm was then converted to percentage for comparison.

Results

Hydraulic Conductivity

Saturated hydraulic conductivity had a nonsignificant depth by land use interaction (p-value = 0.7906), suggesting that although there was a redistribution of topsoil to the bottom of non-uniform hillslopes, the *Ksat* was approximately the same as the uniform hillslopes by depth (Figure 3.6). There was an overall significant effect of depth on *Ksat* (p-value = 0.0088); as the measurement depth increased *Ksat* decreased in magnitude until approximately 175 cm then increased again until 375 cm. This pattern resulted in a quadratic relationship (Equation 4.4) with *Ksat* in cm hr^{-1} and *Depth* in cm.

Equation 4.4

$$\text{Log}(Ksat) = 0.1841585 - 0.0186865 * \text{Depth} + 0.0001594 * (\text{Depth} - 118.678)^2$$

Particle Tracking

The pathways shown by the particle tracker illustrate the soil water flow over the simulation period (1008 days). The flow paths for both models are similar in shape but differ in distance traveled (Figure 3.7). Starting from the ridge, the first two particles for both models run almost directly down to bedrock with the second particle in the non-uniform model moving slightly farther along the bedrock surface towards the seepage face. The shape of the third flow path differed from the first two paths for both models, as the particle moved slightly towards the ridge due to the hydraulic gradient before moving back towards the bedrock. The third particle track path in the uniform model continued for a longer distance along the bedrock than the non-uniform pathway. The flow paths of the fourth particles were similar for both models, but again

the uniform model traveled for a longer distance down slope. Lastly, the fifth particle's pathway for both models had the same shape and length traveled.

Water Flow

Water content (θ) was evaluated for each hillslope model using observation nodes placed within each soil horizon along the seepage face boundary. These nodes were used to estimate the water content contributed to seepage from the whole horizon thickness summed over 1959 and 1960 (Table 3.2). The top two soil horizons contributed 78.4 % and 83.3 % of the water content over the simulation period for the uniform and non-uniform model, respectively (Table 3.2).

Variations in the water content (θ) of the hillslope profiles were compared at the end of the simulation run (Figure 3.7). Water content was highest in the low permeability layer compared to the topsoil and subsoil for each model, as expected from clay's high water holding capacity. The low permeability layer in the uniform model had a water content that was consistently high (approximately 34.7 to 41.0 %), which contrasted with the non-uniform model which that had a lower range of water contents (approximately 25.3 to 37.9 %). Topsoil in both models had a similar trend in the argillic layer, with the water content of the uniform topsoil being about 9.4 % higher than the non-uniform model topsoil.

Water Budget

Infiltration (precipitation), root water uptake, and seepage face flux (Figure 3.8) were used to estimate the percent change in hillslope water storage by year (i.e., 1959 and 1960; Table 3.3). During the first year, both uniform and non-uniform models had a positive change in water storage of 11.0 and 11.6 %, respectively. In the second year, the uniform model showed a loss of

water storage that was two times greater than the amount of storage that had been gained the year before (-11.0 %) meaning over the two years there was a net zero storage. The non-uniform model had a 7.0 % loss of water storage in the second year, which left a positive net soil water storage of 4.6 % over the two-year simulation period.

Discussion

Typically, modeled hillslope hydrology of the Piedmont involves a hydraulically limited layer (argillic horizon) that is parallel to the soil surface that contributes to interflow during periods of high rainfall. Interflow in a hillslope with uniform thickness of topsoil may not represent landscapes that have been disturbed by agriculture, which has resulted in substantial soil redistribution. The objective of this research was to understand the effect of topsoil thickness, particularly redistributed soil to lower hillslope positions, on hillslope interflow. Two hillslope models, with uniform and non-uniform topsoil thicknesses were parameterized with depth to the limiting layer and *Ksat* data quantified from field measurements. Results from comparisons conducted on both depth-to-clay scenarios found that our hypothesis was in part supported and that topsoil thickness does impact interflow.

Hydraulic Conductivity

It was expected that historically farmed landscapes (non-uniform model) that had a redistribution of the topsoil and a deeper depth to the argillic horizon in the lower landscape positions would have low *Ksat* values deeper within the soil profile than the undisturbed hillslopes (uniform model), particularly toward lower slopes positions. Results, however, found an unexpected similarity in *Ksat* by depth. This similarity could be attributed to variation in the

strength of soil structure throughout the low permeability layer or restoration of soil structure during the last 60 years of reforestation (West *et al.*, 2008). Variation or restoration of structure in the upper portion of the limiting layer between undisturbed hillslopes and historically farmed landscapes could create a similar decrease in *Ksat* (1.60 – 36.17 cm hr⁻¹ to 0.01 to 0.32 cm hr⁻¹ near 175 cm) at approximately the same depth. The low *Ksat* data observed in this study was similar to a previous study conducted in the Piedmont of Georgia that found *Ksat* of the limiting layer to range from 0.30 cm hr⁻¹ in the upper portion of the limiting layer to 0.07 cm hr⁻¹ in the lower portion (West *et al.*, 2008). This variance in *Ksat*, as also observed in this study, could obscure patterns with depth over the 40 cm change in thickness with lower slope deposition.

Below the argillic horizon, the measured increase in *Ksat* (0.8 to 19.5 cm hr⁻¹) deeper in the profiles likely results from the coarse textured, sandy subsoil (i.e., BC or CB horizon as characterized in the field), a subsoil that conducts water at a rate comparable to the surface horizon (Figure 3.6). The higher *Ksat* data shown in this study is comparable to another study conducted in the Piedmont that found high *Ksat* values for saprolite at depth with as much as 1.71 cm hr⁻¹ (Vepraskas *et al.*, 1991). *Ksat* measures of saprolite are relatively limited but clearly suggest a higher *Ksat* value than those observed in the limiting layer above.

Particle Tracking and Water Flow

The effect of topsoil thickness on the hydrology of each hillslope, especially interflow, was evaluated both qualitatively (particle tracking) and quantitatively (water content). Particle track flow paths seemed preferential to vertical rather than lateral flow. Given that the years simulated had high rainfall, it was expected that lateral flow would be more prevalent. Although this was not the case, it is worth noting that nearly all flow paths indicated that water exited

through the subsoil at the very base of the seepage face (Figure 3.7). The final location of each particle track is near or on the no-flow bedrock boundary, which suggests that despite the presence of a low permeability layer lateral movement downslope was slower than its vertical movement. Previous studies have reported similar circumstances where percolation through the low permeability, or other macropores (*e.g.*, anomalies created through the limiting layer created by roots) may cause interflow to be infrequent contributing more to vertical movement (Jackson *et al.*, 2014, Du *et al.*, 2016).

Quantitative evaluations of interflow from water flow, estimated as a percentage contributed by each soil horizon at the seepage face boundary over the two-year simulation period, indicated most of the water flux occurred in the top two soil horizons (Table 3.2). This result is contrary to the particle tracking flow paths that exited towards the bottom of the seepage face. This discrepancy could partly result from simulation error. Error associated with the water budgets is apparent in infiltration estimates between the two models despite both models receiving the same precipitation. The non-uniform depth-to-clay model estimated 7.0 cm more infiltration into the hillslope compared to the uniform topsoil model. These 7.0 cm of infiltration missing from the uniform topsoil model is considered to have been runoff. Possibly as a result of this greater infiltration, the non-uniform topsoil experienced a higher water flux than the uniform topsoil, contrary to what was hypothesized. This higher flux at the seepage face could be related to the greater infiltration and steeper slope of the subsoil topography in the non-uniform model. The steeper slope creates less contact time for the infiltrated water to percolate into and through the limiting layer and therefore runs over the limiting layer and exits the hillslope through the topsoil.

In addition to the flux at the seepage face, the water content of the entire hillslope was evaluated at the end of the two-year simulation. Assuming the non-uniform topsoil thicknesses had interflow running off the top of the limiting layer rather than infiltrating into the horizon, less water overall could be stored in the limiting layer (as was seen in the lower ranges of water content compared to the uniform hillslope; Figure 3.7). Sloping subsoil in the non-uniform model may also impact the residence time of the water content in the topsoil, as most of the infiltrated water moved quickly through the sandy topsoil and drained out of the profile seepage face compared to the less sloping topsoil in the uniform model. In the uniform model the infiltration does percolate into the limiting layer thereby contributing a higher water content percentage than the topsoil (Figure 3.7). Residence time of soil water has previously been shown to be highly correlated with topography, with lower residence times associated with more sloping topography (McGuire *et al.*, 2005). Also, partly as an artifact of our model structure, the redistribution of the non-uniform topsoil displaced subsoil from the bottom of the hillslope profile, creating an aquifer-like confining layer in the sandy subsoil, which over time fills with water that moves back up the hillslope along the bedrock. The uniform hillslope does not have this artifact, and more of the water was able to drain out the seepage face which created a dry zone below the limiting layer.

Water budget

Water storage for the first year was similar for both models but may result from different processes (Table 3.3). The uniform model had more water stored in the topsoil and limiting layer but was dryer in the sandy subsoil than the non-uniform model. The coarse saprolite in the Piedmont region has a low water storage capacity (Baloochestani, 2008). Speculatively, the soil

water that percolates through the limiting layer of the uniform model will drain quickly through coarse subsoil, creating a dry zone below the limiting layer. Previous studies have shown that topography controls water storage, with shallower slopes allowing for more infiltrated water to remain in the soil for a longer time than steeper slopes (Boggs *et al.*, 2013). However, the non-uniform model contained more water in the “confined aquifer” making the change in storage similar. In the second year the non-uniform model had 7.0 cm more infiltration than the uniform model; therefore, the higher water storage may have come from the non-uniform model experiencing less runoff.

Conclusion

We hypothesized that interflow would be lower in a pre-disturbance landscape that has a uniform depth-to-clay as well as having less soil water storage due to less topsoil thickness at the lower-slope landscape position. Less soil water storage was observed in the uniform model simulations but model artifacts could have misrepresented water storage as the non-uniform model had “aquifer-like” subsoil water storage. Our hypothesis of less interflow in the uniform hillslope model was not supported. Interflow on top of the limiting layer was higher in the non-uniform model, however, water content within the limiting layer was higher in the uniform model. Although these models do not fully represent the complexities of the heterogeneous nature of soil, the simplifications did offer some insight on how topsoil thickness affected interflow. In our model framework, when topsoil was redistributed (i.e., non-uniform model) subsoil topography became steeper allowing less soil water to percolate into the limiting layer compared to the uniform topsoil thickness. Further studies comparing hillslopes with soil redistribution may find benefit in evaluating interflow using 1) water flowing on top of the

limiting layer, 2) water flowing within the limiting layer, and 3) retaining constant argillic horizon steepness.

References

- Ali, G. A., L'Heureux, C., Roy, A. G., Turmel, M.-C., & Courchesne, F. (2011). Linking spatial patterns of perched groundwater storage and stormflow generation processes in a headwater forested catchment. *Hydrological Processes*, 25(25), 3843-3857. doi:10.1002/hyp.8238
- Amoozegar, A. (1989). A Compact Constant-Head Permeameter for Measuring Saturated Hydraulic Conductivity of the Vadose Zone. *Soil Science Society of America Journal*, 53(5), 1356-1361. doi:10.2136/sssaj1989.03615995005300050009x
- Baloochestani, F. (2008). Estimation of Hydraulic Properties of the Shallow Aquifer System for Selected Basins in the Blue Ridge and the Piedmont Physiographic Provinces of the Southeastern U.S. Using Streamflow Recession and Baseflow Data. Georgia State University College of Art and Sciences Doctoral Dissertation
- Boggs, J., Sun, G., Jones, D., & McNulty, S. (2013). Effect of soils on water quantity and quality in piedmont forested headwater watersheds of North Carolina. *Journal of the American Water Resources Association*, 49(1), 132-150.
- Brecheisen, Z., Cook, C., & Harmon, M. (2015). US Forest Service Photograph from the Photographic Archive of the Calhoun Experimental Forest, <http://criticalzone.org/calhoun/data/dataset/4324/>.
- Chaplot, V., & Walter, C. (2003). Subsurface topography to enhance the prediction of the spatial distribution of soil wetness. *Hydrological Processes*, 17(13), 2567-2580. doi:10.1002/hyp.1273
- Dialynas, Y. G., Bastola, S., Bras, R. L., Billings, S. A., Markewitz, D., & Richter, D. d. (2016). Topographic variability and the influence of soil erosion on the carbon cycle. *Global Biogeochemical Cycles*, 30(5), 644-660. doi:10.1002/2015GB005302
- Dreps, C. L. (2011). Water Storage Dynamics and Water Balances of Two Piedmont North Carolina Headwater Catchments (Master's Thesis). NC State University, Raleigh, North Carolina.

- Du, E., Jackson, C. R., Klaus, J., McDonnell, J. J., Griffiths, N. A., Williamson, M. F., Greco, J. L., & Bitew, M. (2016). Interflow dynamics on a low relief forested hillslope: Lots of fill, little spill. *Journal of Hydrology*, 534, 648-658.
- Feddes, R. A., Kowalik, P. J., & Zaradny, H. (1978). *Simulation of field water use and crop yield*: Centre for Agricultural Publishing and Documentation.
- Gabbard, D., Huang, C., Norton, L., & Steinhardt, G. (1998). Landscape position, surface hydraulic gradients and erosion processes. *Earth Surface Processes and Landforms*, 23(1), 83-93.
- GoogleMaps. (2017). Sumter National Forest, <https://www.google.com/maps/search/sumter+national+forest/@34.1570253,-83.4621966,7z/data=!3m1!4b1>.
- Huang, C., Gascuel-Oudou, C., & Cros-Cayot, S. (2002). Hillslope topographic and hydrologic effects on overland flow and erosion. *CATENA*, 46(2-3), 177-188. doi:[http://dx.doi.org/10.1016/S0341-8162\(01\)00165-5](http://dx.doi.org/10.1016/S0341-8162(01)00165-5)
- Jackson, C. R., Bitew, M., & Du, E. (2014). When interflow also percolates: downslope travel distances and hillslope process zones. *Hydrological Processes*, 28(7), 3195-3200.
- McGuire, K. J., McDonnell, J. J., Weiler, M., Kendall, C., McGlynn, B. L., Welker, J. M., & Seibert, J. (2005). The role of topography on catchment-scale water residence time. *Water Resources Research*, 41(5), n/a-n/a. doi:10.1029/2004WR003657
- NCEI. (2016). NOAA National Center of Environmental Information, <https://www.ncei.noaa.gov/>
- O'loughlin, E. (1981). Saturation regions in catchments and their relations to soil and topographic properties. *Journal of Hydrology*, 53(3-4), 229-246.
- Paniconi, C., & Wood, E. F. (1993). A detailed model for simulation of catchment scale subsurface hydrologic processes. *Water Resources Research*, 29(6), 1601-1620.

- Qi, J. (2016). Potential Climate Change Effects on Deep Soil Carbon and Hydrology in Loblolly Pine Plantations of the Southeast US (Doctoral Dissertation). University of Georgia. Athens, GA.
- Quinn, P., Beven, K., Chevallier, P., & Planchon, O. (1991). The prediction of hillslope flow paths for distributed hydrological modelling using digital terrain models. *Hydrological Processes*, 5(1), 59-79.
- Richards, L. A. (1931). Capillary conduction of liquids through porous mediums. *Physics*, 1(5), 318-333.
- Richter, D. D., Bacon, A. R., Billings, S. A., Binkley, D., Buford, M., Callahan, M. A., Curry, A. E., Fimmen, R. L., Grandy, A. S., Heine, P. R., Hofmockel, M., Jacks, J. A., LeMaster, E., Li, J., Markewitz, D., Mobley, M. L., Morrison, M. W., Strickland, M. S., Waldrop, T., and Wells, C. G., (2015). *Evolution of soil, ecosystem, and critical zone research at the USDA FS Calhoun Experimental Forest* (Vol. 18).
- Richter, D. D., & Markewitz, D. (2001). *Understanding soil change: soil sustainability over millennia, centuries, and decades*: Cambridge University Press.
- Schaap, M. G., & Leij, F. J. (1998). Using neural networks to predict soil water retention and soil hydraulic conductivity. *Soil and Tillage Research*, 47(1), 37-42.
- Schaap, M. G., Leij, F. J., & Van Genuchten, M. T. (2001). ROSETTA: a computer program for estimating soil hydraulic parameters with hierarchical pedotransfer functions. *Journal of Hydrology*, 251(3), 163-176.
- Šimůnek, J., van Genuchten, M. T., & Šejna, M. (2016). Recent developments and applications of the HYDRUS computer software packages. *Vadose Zone Journal*, 15(7).
- Trimble, S. W. (1974). Man-induced soil erosion on the southern Piedmont. *Soil Conserv. Soc. Am., Ankeny, Iowa*, 1700-1970.
- Van Genuchten, M. T. (1987). *A numerical model for water and solute movement in and below the root zone*: United States Department of Agriculture Agricultural Research Service US Salinity Laboratory.

Vepraskas, M. J., Hoover, M. T., Jongmans, A. G., & Bouma, J. (1991). Hydraulic Conductivity of Saprolite as Determined by Channels and Porous Groundmass. *Soil Science Society of America Journal*, 55(4), 932-938. doi:10.2136/sssaj1991.03615995005500040006x

Wang, J., Shen, Y., & Shahnaz, S. (2015). Calhoun Experimental Forest-Stream Flow and Rainfall

West, L. T., Abreu, M. A., & Bishop, J. P. (2008). Saturated hydraulic conductivity of soils in the Southern Piedmont of Georgia, USA: Field evaluation and relation to horizon and landscape properties. *CATENA*, 73(2), 174-179.
doi:<https://doi.org/10.1016/j.catena.2007.07.011>

Table 3.1. Soil water retention parameters for hillslope hydraulic models with uniform and non-uniform topsoil thicknesses. Saturated hydraulic conductivity (K_{sat}) was measured on site, residual volumetric water content (θ_r), saturated volumetric water content (θ_s), and the water retention functions α and n were estimated in HYDRUS.

Soil Horizon	Soil Texture	θ_r (cm^3/cm^3)	θ_s (cm^3/cm^3)	α (1/cm)	n (-)	K_s (cm/day)
Surface	Sandy Loam	0.065	0.41	0.075	1.89	530
Hydrologically Limiting	Clay	0.095	0.41	0.019	1.31	4
Sub-Limiting	Sandy Loam	0.065	0.41	0.075	1.89	530

Table 3.2. Water content contributed by soil horizon for models with uniform and non-uniform topsoil thicknesses. Water flow measurements from a single observation point within each horizon at the seepage face were used as estimates for the water flow contributed by each horizon over the simulation run presented here as each horizon's percentage of the total.

Soil Horizon	Uniform (%)	Non-Uniform (%)
Surface	28.5	42.5
Hydrologically Limiting	49.9	40.8
Sub-Limiting	21.6	16.7

Table 3.3. Percent hillslope soil water storage for models with uniform and non-uniform topsoil thicknesses. Soil water storage was calculated with daily data from January to December for 1959 and 1960 in the Calhoun Critical Zone Observatory, SC.

Year	Boundary Flux	Uniform (cm)	Non-uniform (cm)
1959	Infiltration	143.0	142.5
	Root Water Uptake	89.2	95.2
	Seepage Face Flux	38.0	31.1
	Change in Storage	13.8	16.2
1960	Infiltration	130.6	137.5
	Root Water Uptake	91.4	94.2
	Seepage Face Flux	53.5	53.7
	Change in Storage	-14.3	-10.4

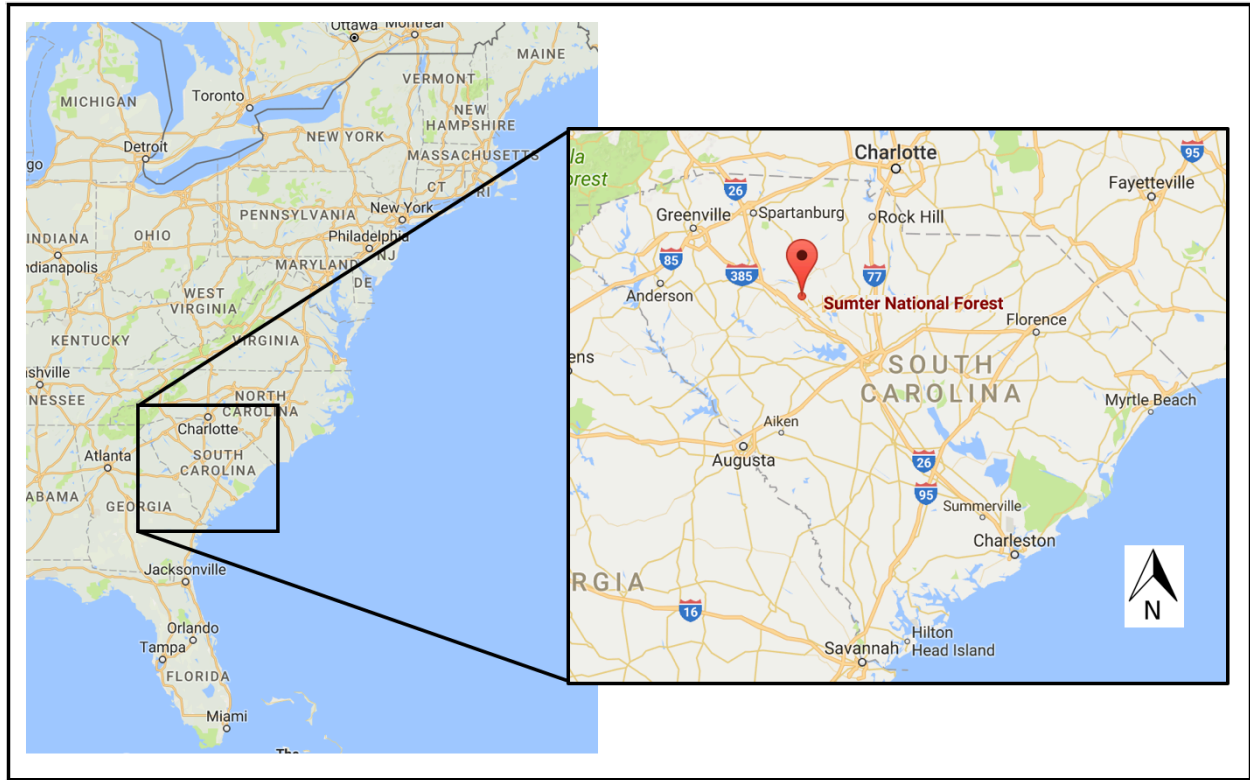


Figure 3.1. Location of the Calhoun Critical Zone Observatory in the Sumter National Forest, SC.

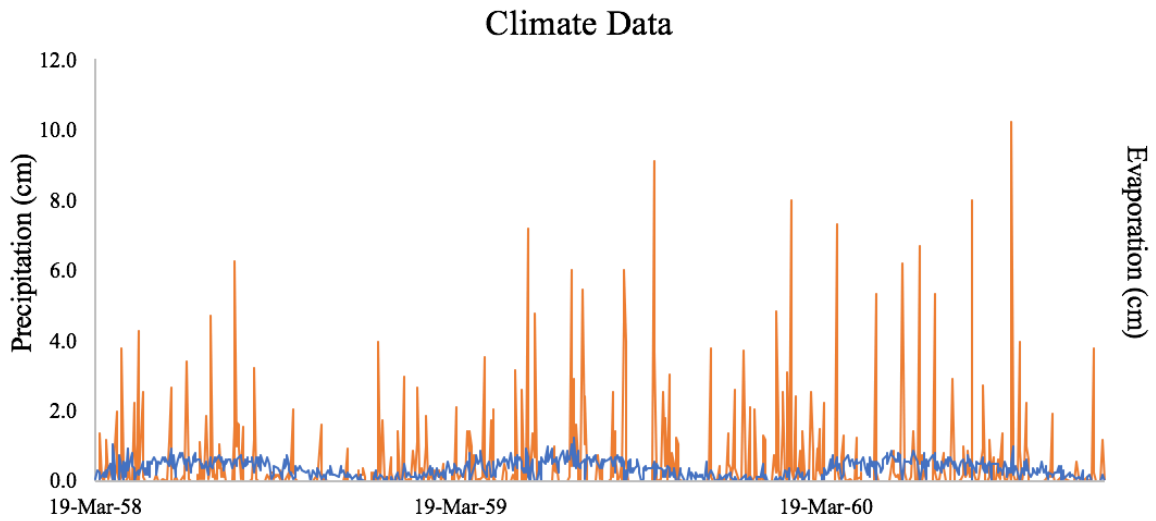


Figure 3.2. Precipitation (orange) collected from the Calhoun Critical Zone Observatory (CCZO), and evapotranspiration (blue) collected from weather station near the CCZO for March 1958 to December 1960. Years 1958 - 1960 were chosen due to the high precipitation inputs for the year.

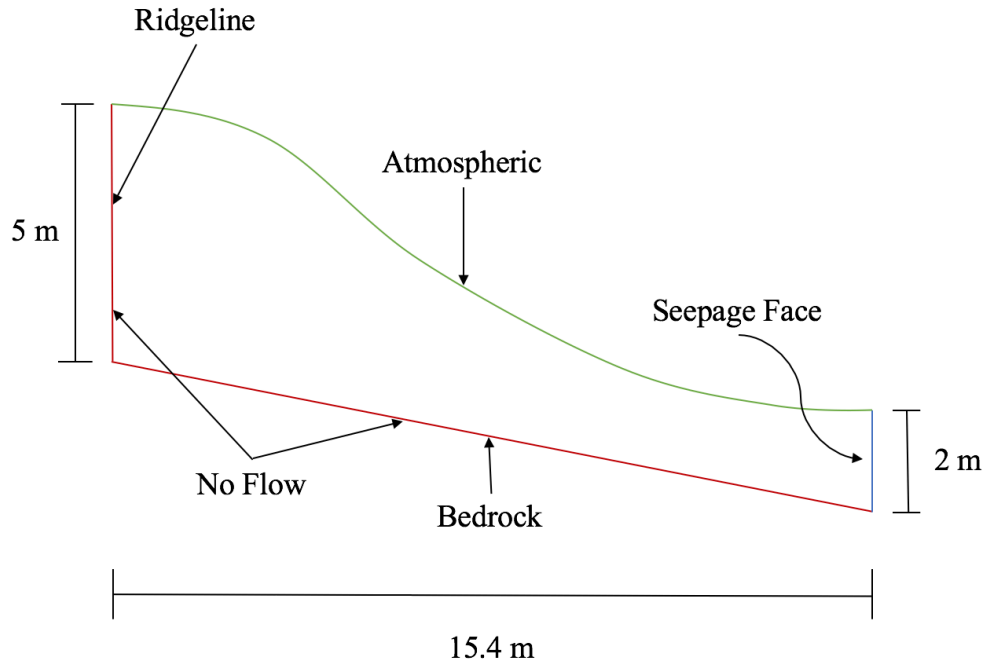


Figure 3.3: Boundary conditions and dimensions for vertical hillslope cross section. The ridgeline (along the left-hand side) and bedrock (along the bottom of the modeling space) are represented as no flow boundaries (red lines), the atmospheric boundary is along the soil surface (green line), and the hillslope drainage occurs at the seepage face (blue line).

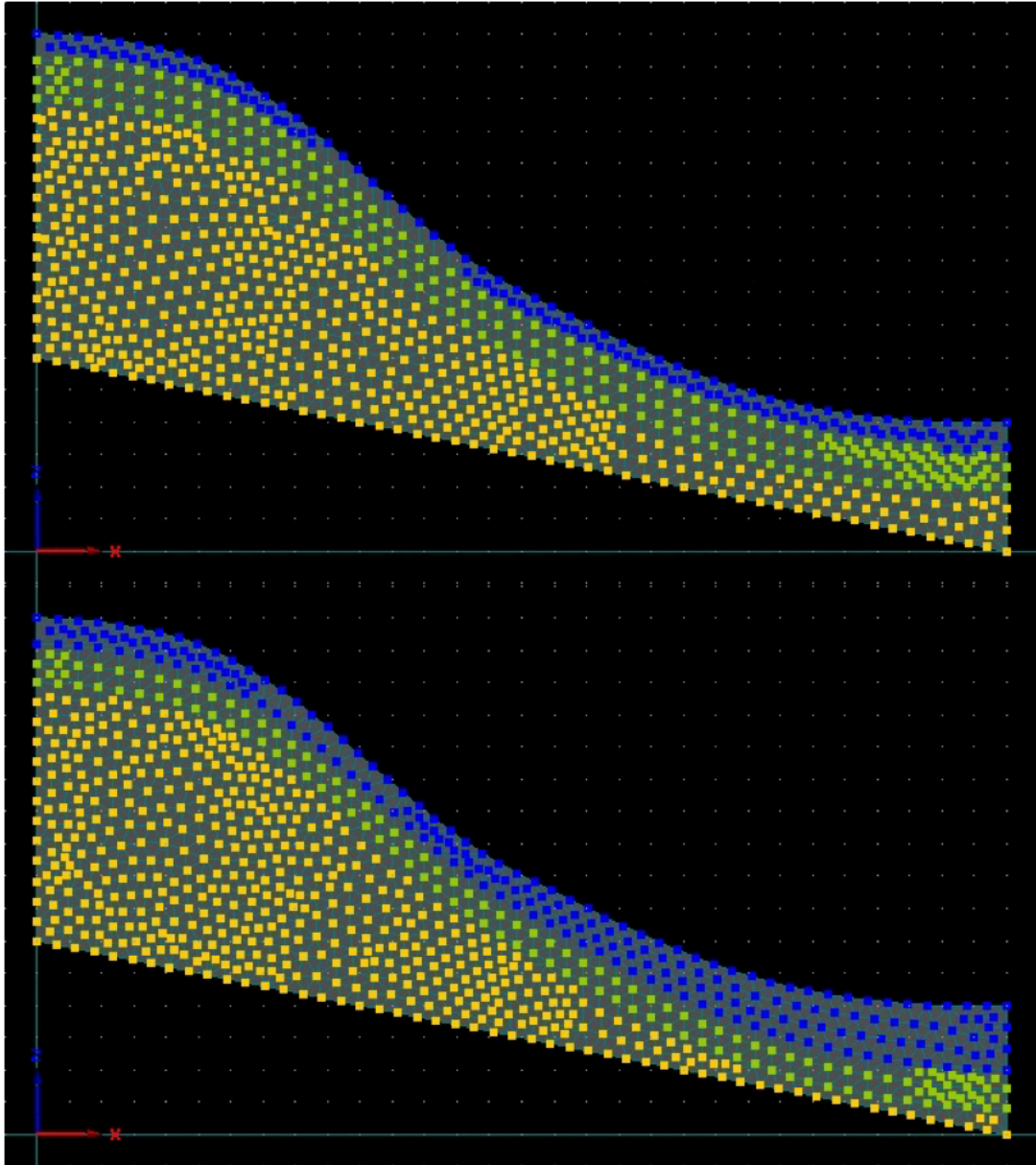


Figure 3.4: Hillslope soil profile layers for both uniform (top) and non-uniform (bottom) thickness of topsoil. The thickness of the sandy topsoil layer (blue) is consistently 40 cm for the uniform hillslope and 40 cm at the ridge, 50 cm at the mid-slope, and 80 cm at the toe-slope for the non-uniform model. The low permeable clay layer (green) is 60 cm thick for both models, and the sandy subsoil (yellow) fills the rest of the modeling space. Depths of each soil layer were determined from Figure 2.4.

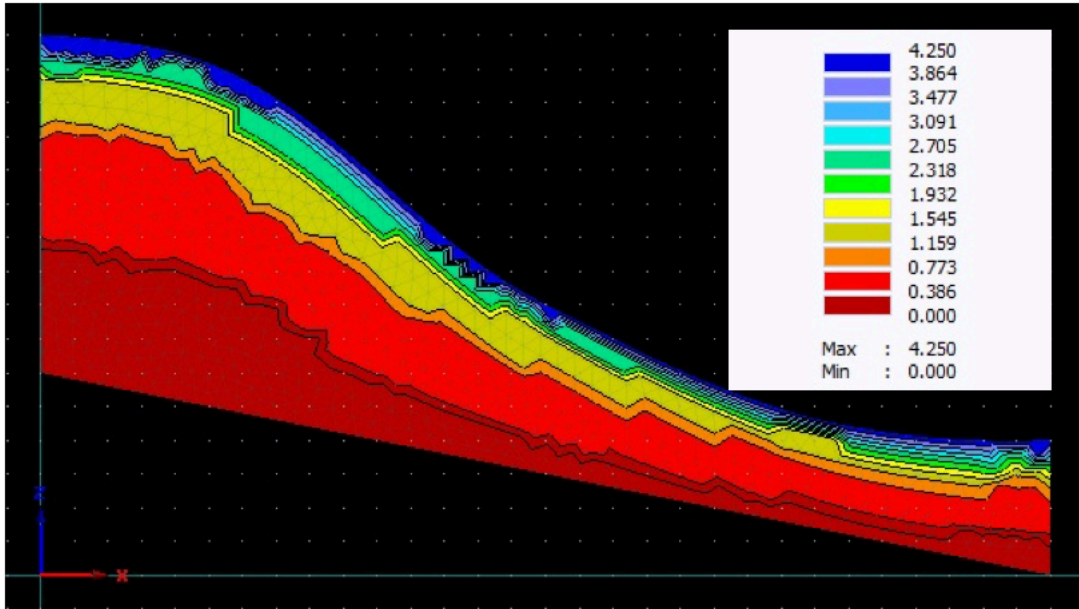


Figure 3.5: Exponential decrease in rooting distribution for both uniform and non-uniform topsoil thickness models. A higher density of roots is located along the soil surface (blue) and decreases with depth (red).

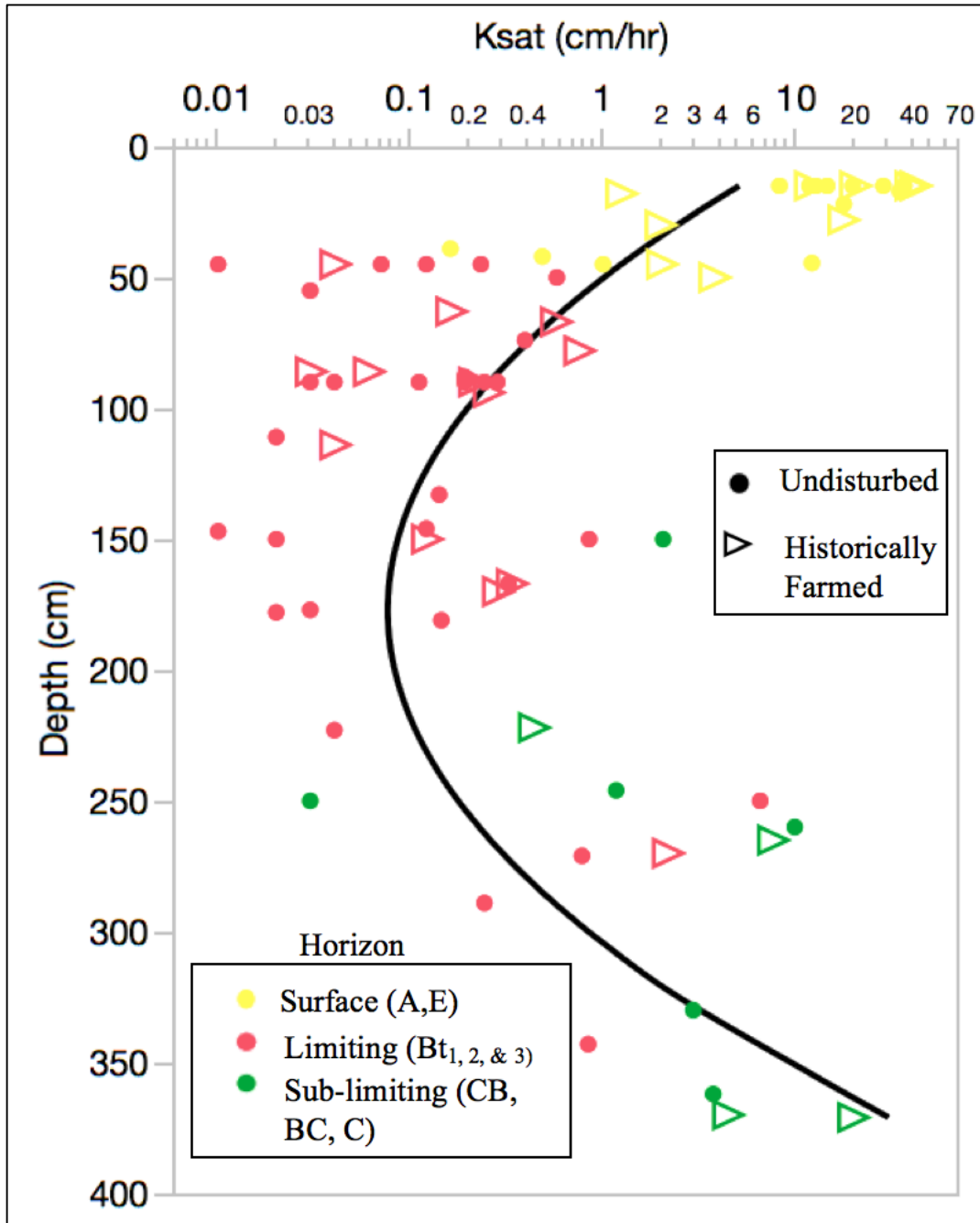


Figure 3.6: Saturated hydraulic conductivity (K_{sat}) measured in 2017 in the Calhoun Critical Zone Observatory, SC on landscapes with uniform and non-uniform thickness of topsoil.

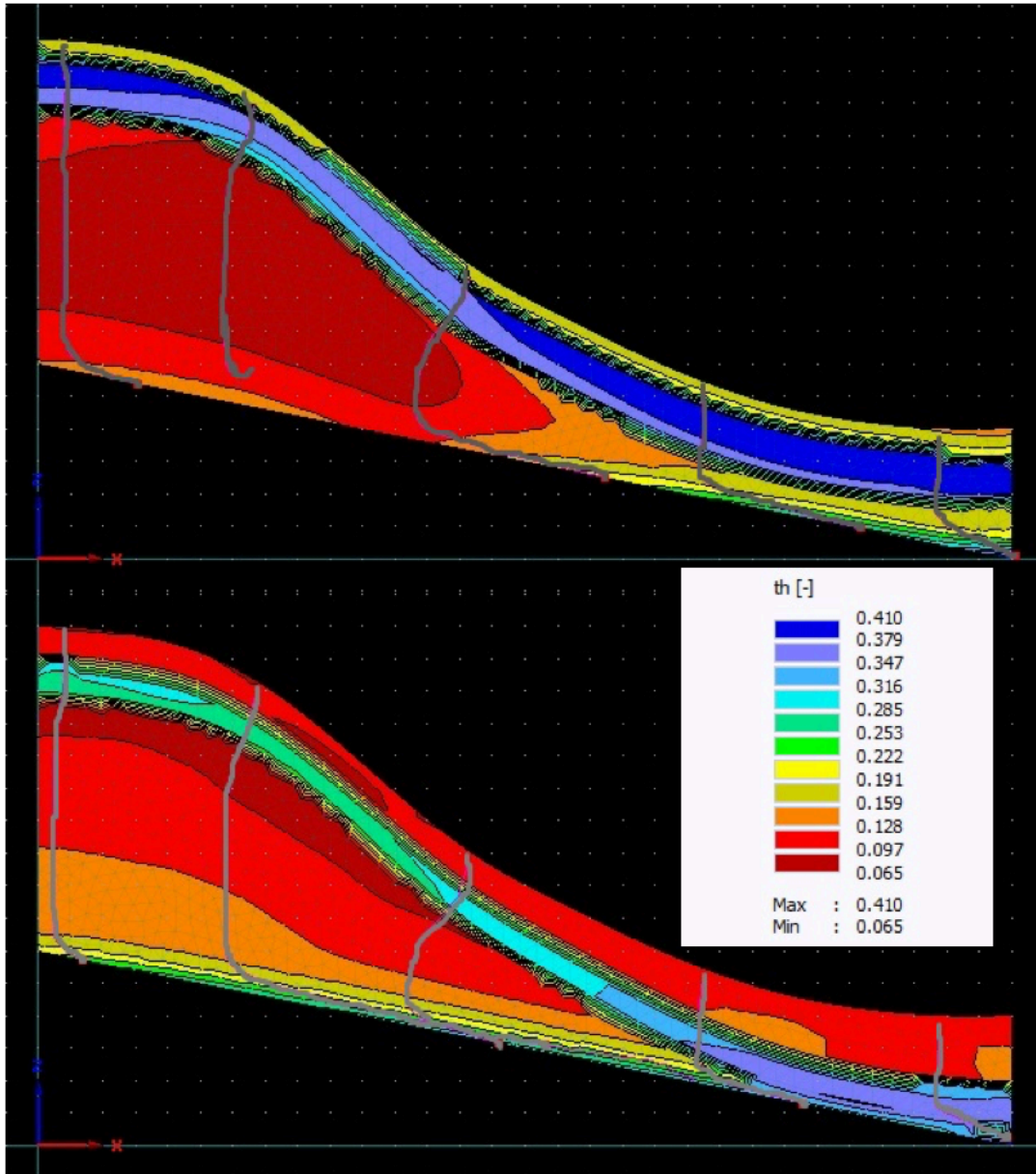


Figure 3.7: Vertical hillslope cross section with particle tracking (grey lines) of interflow, over a two-year simulation, for models with uniform (top) and non-uniform (bottom) topsoil thicknesses. Background colors represent variations in water content (θ) at the end of the 1008-day simulation. Higher water content has a blue color whereas lower water content has a red color.

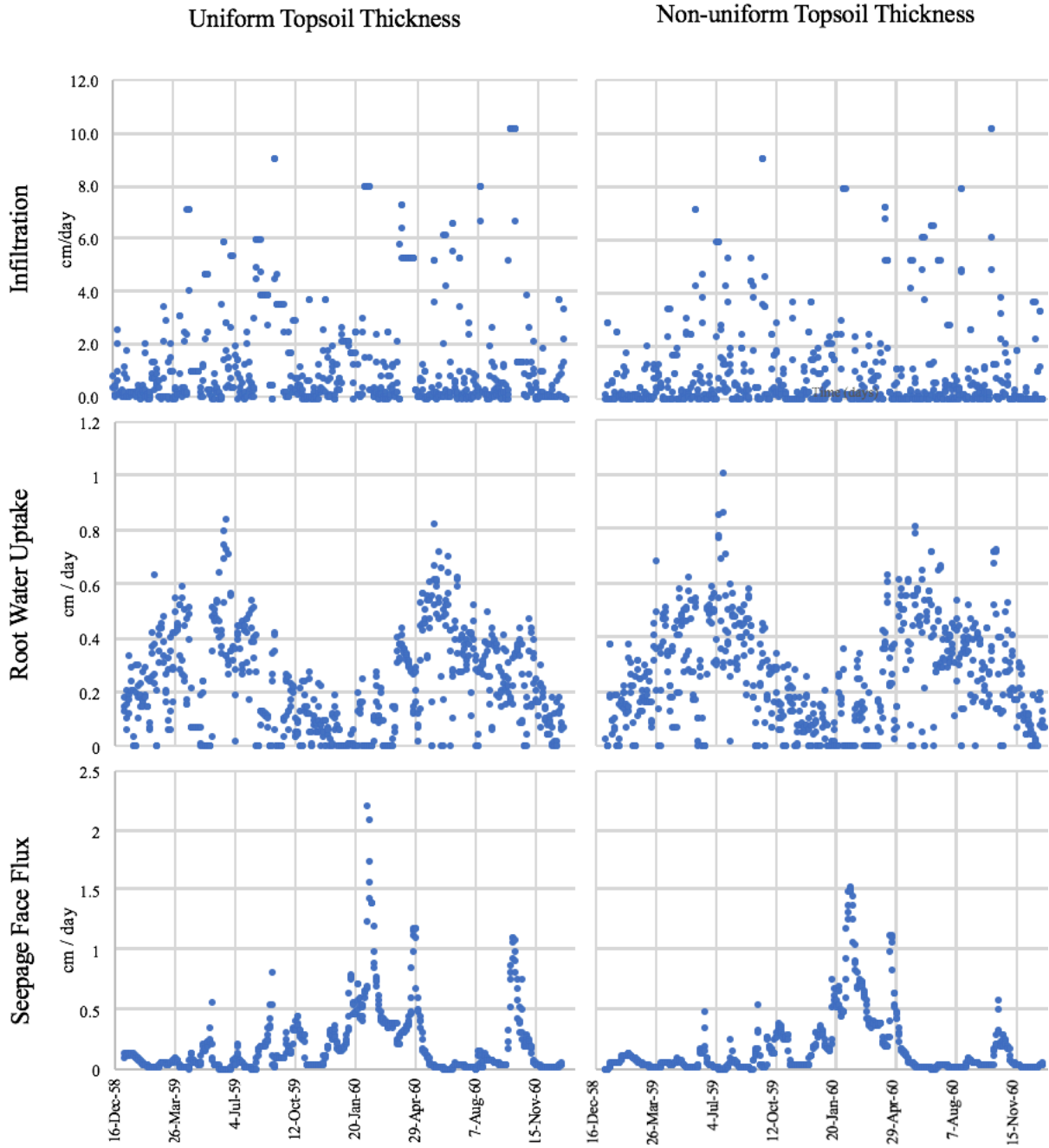


Figure 3.8: Simulated daily infiltration, root water uptake, and seepage face flux used to calculate soil water storage for models with uniform and non-uniform topsoil thickness. Data are for two years, January 1st to December 30th, 1959 and 1960.

CHAPTER 4

CONCLUSION

Spatial variations in the depth to the argillic horizon as categorized by soil surveys maps, may not accurately represent landscapes in the Southeastern Piedmont that have been effected by severe erosion. This study found that the depth to the argillic horizon was significantly different between landscapes with contrasting land use histories. Landscapes with a history of farming experienced soil redistribution from upper to lower landscape positions contributing to 40 cm soil on average in the toe-slope than land areas that had not been disturbed by agriculture (having a consistent depth to the argillic horizon along the hillslope). The depth to the argillic horizon as determined by tile push probe (TPP) and soil boring was not well predicted by regression efforts on the undisturbed hillslope with a consistent depth to clay ($R^2 = 0.24$). The TPP, however, did correlated strongly with soil boring observations for historically farmed watersheds ($R^2 = 0.80$). Combining soil boring and TPP techniques allowed for an extensive investigation of the spatial variation in the depth to the argillic horizon along hillslope profiles.

When assessing the potential use of geophysical sensing (specifically EMI) as a means of measuring the depth to the argillic horizon in forested landscape our results showed that electrical conductivity alone was not a strong predictor of the depth to the clay layer ($R^2 = 0.31$). The strength of the prediction increased, however, with the addition of regression kriging (RK) with other landscape features variables (*i.e.*, slope, and landscape position) ($R^2 = 0.71$). These improved predictors can be related back to land use history. In general, RK did performed well in predicting the variation in depth-of-clay, capturing both the large variation in the historically

farmed and the more limited depth in the reference hillslopes. Additionally, the results of the RK predicted maximum depths to the argillic layer which were similar to those reported for each land use.

The depth to the argillic horizon is typically parallel to the soil surface in modeled hillslope hydrology of the Piedmont, however, watersheds with soil redistributed to lower landscape positions are less represented. This study found that topsoil thickness, as modeled by uniform and non-uniform depth to the argillic horizon, does impact interflow. Quantitative evaluations of interflow as estimated as a percentage contributed by each soil horizon at the seepage face boundary indicated most of the water flux occurred in the top two soil horizons, with non-uniform topsoil having a higher flux. This higher flux at the seepage face was contributed by greater infiltration and steeper slope of the subsoil topography than the uniform model. Less soil water storage was observed in the uniform model simulations but model artifacts could have misrepresented water storage as the non-uniform model had “aquifer-like” subsoil water storage. When topsoil was redistributed, topography became steeper allowing less soil water to percolate into the hydrologically limiting layer compared to the uniform topsoil thickness. This study also found that saturated hydraulic conductivity (K_{sat}) was approximately the same for both uniform and non-uniform depth-to-clay landscapes by depth. As the measurement depth increased, K_{sat} decreased until approximately 175 cm then increased again until 375 cm. This similarity could be attributed to variation in the strength of soil structure throughout the low permeability layer or restoration of soil structure during the last 60 years of reforestation.

Although these models did not fully represent the complexities of the heterogeneous nature of soil, the simplifications did offer some insight on how topsoil thickness affected

interflow. Accelerated erosion contributed to soil redistribution and thicker topsoil in lower landscape positions due to historical agricultural practices. Time and cost limit the extent of direct soil sampling; therefore, landscapes, such as those in the Piedmont region of the southeastern USA, that have been altered by historic agricultural land use are often misrepresented.

APPENDIX A

ORGANIC MATTER PRETREATMENT

Introduction

When conducting particle size analysis, organic matter can inhibit complete dispersion of the sample and therefore effect the predicted textural class (Jensen *et al.*, 2017). There are many pretreatment methods to remove organic matter including heat and chemical (Gee *et al.*, 1986). Heat treatment, however, can cause clay particles to cement when exposed to prolonged heat (550°C) creating a texture analysis that is coarser than expected (Vaasma, 2008). Therefore, a chemical treatment is preferred. Hydrogen peroxide is a common chemical treatment used when removing organic matter and was used here.

Method

An organic matter removal experiment was conducted on 9 soil samples ranging in depth from 0 – 100 cm. Soil samples were collected in watershed 3 and 4 of the Calhoun Experimental Forest. Samples were prepared according to method in Chapter 2 methods. Sample were heated to approximately 60°C and treated with hydrogen peroxide until frothing ended and soil appeared to be bleached (Figure A.1). Texture analysis was then conducted on samples with and without organic matter (Gee *et al.*, 2002).

Results

A 1 to 1 correlation of percent clay in samples, ranging in depth from 0 – 100 cm, with and without organic matter removal (Figure A.2). Generally, clay content is under estimated when organic matter is present. The root mean squared error of the correlation is 2.122 percent. Since the relationship of clay content with and without organic matter was strong, the remaining samples collected for the project discussed in Chapter 2 were not pretreated with hydrogen peroxide.

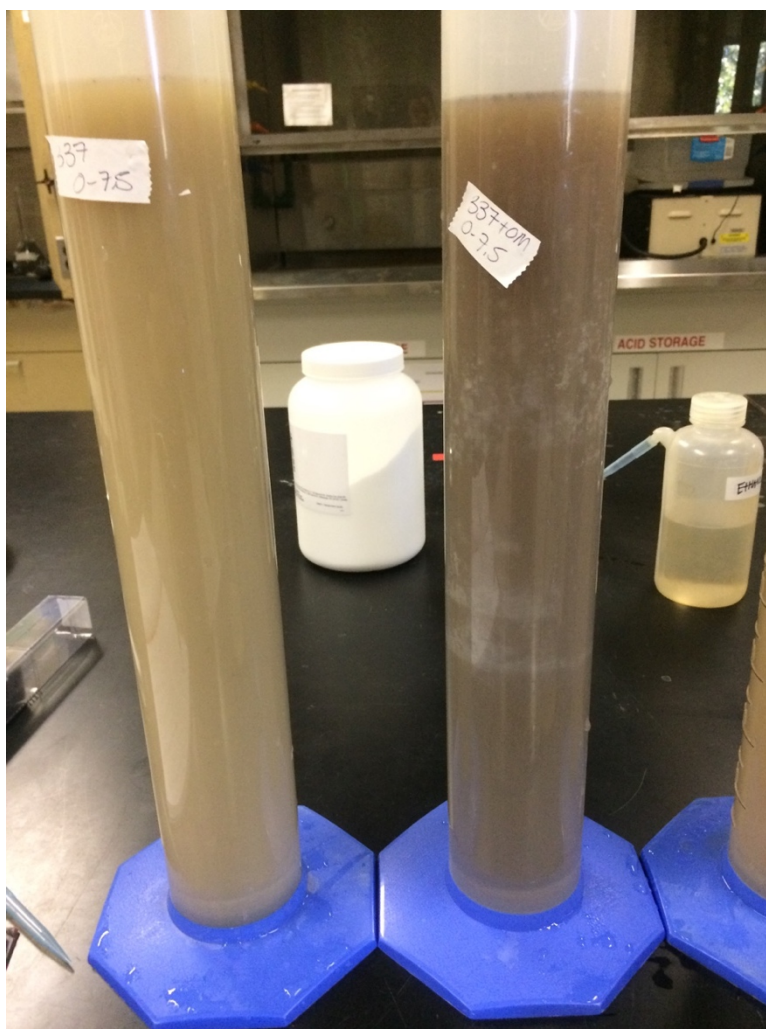


Figure A.1: Soil sample with organic matter (right) and same sample that has been treated with hydrogen peroxide and now appears “bleached” (left).

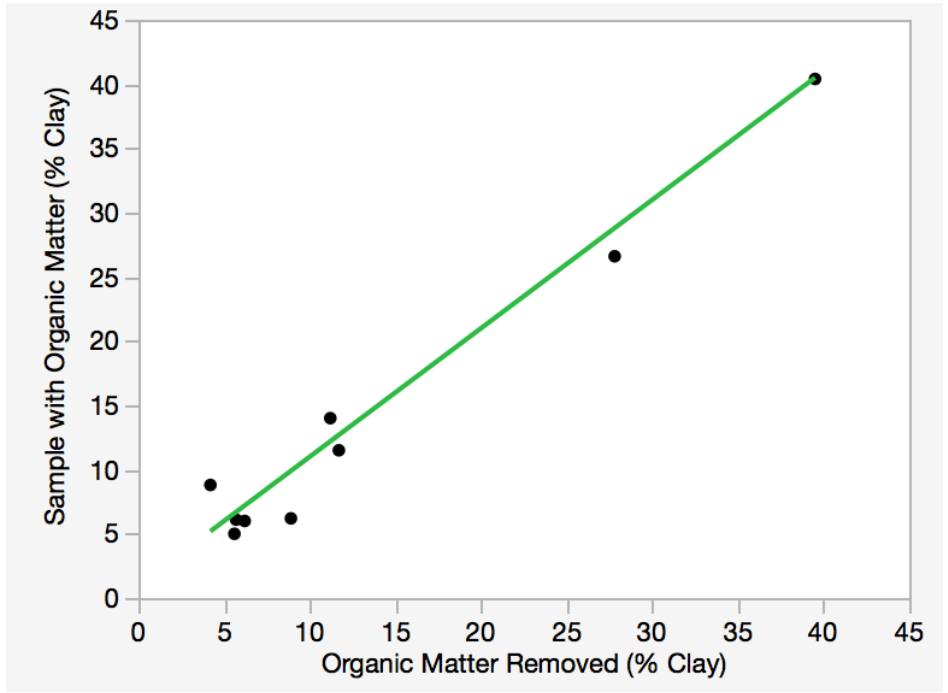


Figure A.2: 1 to 1 correlation of percent clay between samples with organic matter and samples without organic matter (n=9).

APPENDIX B

CROSS VALIDATION OF ORDINARY KRIGING FOR GEOPHYSICAL SENSING DATA

Method

A simple cross validation, using 10 % of the geophysical sensing data (EMI), was conducted on the twenty ordinary kriged surfaces, to test performance. Two metrics were utilized, mean squared deviation ratio (MSDR)

$$MSDR = \frac{1}{N} \sum_{i=1}^N \frac{\{z(x_i) - \hat{Z}(x_i)\}^2}{\hat{\sigma}_K^2(x_i)} \quad \text{Equation B.1:}$$

and root mean squared error (RMSE)

$$RMSE = \left[\frac{1}{N} \sum_{i=1}^N \frac{\{z(x_i) - \hat{Z}(x_i)\}^2}{\hat{\sigma}_K^2(x_i)} \right]^{\frac{1}{2}} \quad \text{Equation B.2:}$$

to assess the fit and accuracy of the semi-variogram to the geophysical sensing data. Equation B.1: $z(x_i)$ is the i^{th} observed geophysical sensing value set aside for cross validation at x_i , $\hat{Z}(x_i)$ is the kriged predicted geophysical sensing value at x_i and $\hat{\sigma}_K^2(x_i)$ is the mean squared prediction error (Oliver *et al.*, 2014). Equation B.2: is the square root of Equation B.1 (De Benedetto *et al.*, 2012).

Results

Cross validation of the twenty kriged maps created using ten percent of the data showed that reference 9 performed best (Table B.1). Equations B.1 and B.2 were used to test the fit of the variogram model to the data, as well as the accuracy of the kriged maps. Values for MSDR and RMSE should be close to one. Ordinary kriging with a spherical variogram model was chosen with anisotropy set to true. The range of MSDR and RMSE was 0.084 to 1.988 and 0.291 to 1.410, respectively. Indicating that the fit of the variogram model and the accuracy of the prediction showed large variation in results. H 2 EMI orientations under performed in model fit and accuracy with an average MSDR of 0.6915 (± 0.711 SD) and RMSE of 0.665 (± 0.400 SD). All other EMI orientations performed well, and H1 performed best with an average MSDR and RMSE of 0.895 (± 0.271 SD) and 0.931 (± 0.175 SD), respectively. Reference 9 had the best fit and accuracy for all EMI orientations with an average MSDR and RMSE of 0.897 (± 0.218 SD) and 0.939 (± 0.121 SD), respectively.

Discussion

Cross validation of measured versus predicted electrical conductivity showed how well ordinary kriging (OK) using a spherical variogram, fit the geophysical sensing data for each EMI sensor orientation at each study site and the resulting accuracy of that fit. Due to OK being a popular choice when interpolating soil properties (Saey *et al.*, 2009; Saey *et al.*, 2011; Heil *et al.*, 2012; White *et al.*, 2012) it was expected to perform well. Overall, OK was a good fit, and provided accurate results for 3 of the 4 EMI orientations as well 4 of the 5 study sites. Reference 4 underperformed in both fit and accuracy, this may be due to a small sample size, $n = 27$ (Reference 2 $n = 32$, and Reference 9 $n = 43$). If the sample size were to increase, decreasing

lag size, the prediction may increase over shorter-range variation (Oliver *et al.*, 2014).

Anisotropy may have been a factor as well; again Reference 4 was the smallest of all study sites where anisotropy may not have been present, therefore, unnecessary to use in the model (Oliver *et al.*, 2014).

Table B.1: Cross validation of twenty ordinary kriged surfaces using geophysical sensing data (EMI) for historically farmed watersheds and reference hillslopes; Mean Squared Deviation Ratio (MSDR) and Root Mean Squared Deviation Ratio (RMSR).

Site	EMI Orientation	MSDR	RMSE
Watershed 3	H1	1	1
	P1	1.315	0.847
	H2	0.144	0.397
	P2	1.003	0.482
Watershed 4	H1	1	1
	P1	0.647	0.419
	H2	0.239	0.488
	P2	0.855	0.925
Reference 2	H1	0.996	0.998
	P1	0.441	0.664
	H2	1.988	1.41
	P2	1.587	1.26
Reference 9	H1	1.118	1.057
	P1	0.879	0.937
	H2	0.55	0.742
	P2	1.042	1.02
Reference 4	H1	0.361	0.601
	P1	1.012	1.005
	H2	0.084	0.291
	P2	0.264	0.514

APPENDIX C

SAVANNAH RIVER SITE

Introduction and Site Description

In addition to research at the Calhoun, calibration of the EMI instrument was also conducted at the U.S. Department of Energy's Savannah River Site (SRS) located in the Coastal Plain of South Carolina. This site has Ultisols with a homogenous sandy capped argillic horizon, which provides a more discrete textural contrast for calibrating EMI, as the electrical conductivity between the two horizons is distinct. Previous research showed success (93 % correlation) when predicting the depth to the argillic horizon using electrical conductivity on a similar landscape type in Belgium where there is a homogenous loess capped argillic soil (Saey *et al.*, 2011).

Method

The EMI survey for SRS including the soil boring samples, tile push probe (TPP), and spatial analysis were measurements and collected using the same method discussed in Chapter two methods. Due to thick understory growth, the height at which the EMI was held above the ground increased to 80 cm. Using the method discussed in Saey *et al.* (2011) a cumulative response curve was created for the SRS site. However, there was not enough variation in the depth to the argillic horizon at the SRS for the Saey's method to be successful. Therefore, a secondary spatial error model was conducted in GeoDa (University of Chicago, IL). A distance

weights matrix was created using the Weights Manager option which found the optimal threshold distance based on the dataset.

Results

The EMI orientation for the shallowest depth of exploration P1 was removed from the dataset since the height above the ground was increased the P1 receiver did not measure the soil. The SRS model for predicting the depth to the argillic horizon was significant ($R^2 \geq 60$ and $p \leq 0.15$) as seen in Table C.1. However, it was not significantly different than the spatial models for the heterogeneous sandy capped argillic horizon of Calhoun. The average depth to the argillic horizon, from soil cores observations, was $42.01 \text{ cm} \pm 6.07 \text{ cm}$.

Table C.1: A spatial error model for the Savannah River Site. The dependent variable is depth to the argillic horizon determined by soil core investigation (n=5) and tile push probe measurements (n=35). The explanatory variables are aspect in degrees, slope in percent, EMI sensor orientation H1 and H2 with no transformations.

Depth to Argillic Horizon	Estimator	Std. Error	P-value		
Intercept	12.7112	2.30413	0		
Aspect	-0.022041	0.0081145	0.0066		
Slope	9.27E-06	3.34E-06	0.00554	R ² =	0.66
H2	14.7269	2.77377	0	AIC=	279.83
H1	2.26407	0.646004	0.00046		
Lambda	-0.578018	0.125745	0		